





# The replicative helicase MCM recruits cohesin acetyltransferase ESCO2 to mediate centromeric sister chromatid cohesion

Miroslav P Ivanov<sup>1,†</sup> , Rene Ladurner<sup>1,‡</sup>, Ina Poser<sup>2</sup>, Rebecca Beveridge<sup>1</sup>, Evelyn Rampler<sup>1,§</sup> , Otto Hudecz<sup>3</sup>, Maria Novatchkova<sup>1</sup>, Jean-Karim Hériché<sup>4</sup>, Gordana Wutz<sup>1</sup>, Petra van der Lelij<sup>1</sup>, Emanuel Kreidl<sup>1,¶</sup>, James RA Hutchins<sup>1,††</sup>, Heinz Axelsson-Ekker<sup>5</sup>, Jan Ellenberg<sup>4</sup>, Anthony A Hyman<sup>2</sup>, Karl Mechtler<sup>1,3</sup>  & Jan-Michael Peters<sup>1,\*</sup> 

## Abstract

Chromosome segregation depends on sister chromatid cohesion which is established by cohesin during DNA replication. Cohesive cohesin complexes become acetylated to prevent their precocious release by WAPL before cells have reached mitosis. To obtain insight into how DNA replication, cohesion establishment and cohesin acetylation are coordinated, we analysed the interaction partners of 55 human proteins implicated in these processes by mass spectrometry. This proteomic screen revealed that on chromatin the cohesin acetyltransferase ESCO2 associates with the MCM2-7 subcomplex of the replicative Cdc45-MCM-GINS helicase. The analysis of ESCO2 mutants defective in MCM binding indicates that these interactions are required for proper recruitment of ESCO2 to chromatin, cohesin acetylation during DNA replication, and centromeric cohesion. We propose that MCM binding enables ESCO2 to travel with replisomes to acetylate cohesin complexes in the vicinity of replication forks so that these complexes can be protected from precocious release by WAPL. Our results also indicate that ESCO1 and ESCO2 have distinct functions in maintaining cohesion between chromosome arms and centromeres, respectively.

**Keywords** acetylation; cohesin; DNA replication; ESCO1; replisome

**Subject Categories** Cell Cycle; Chromatin, Epigenetics, Genomics & Functional Genomics; DNA Replication, Repair & Recombination

**DOI** 10.15252/emboj.201797150 | Received 16 April 2017 | Revised 27 February 2018 | Accepted 9 April 2018 | Published online 21 June 2018

**The EMBO Journal (2018) 37: e97150**

## Introduction

Chromosome segregation depends on sister chromatid cohesion, which enables the bi-orientation of chromosomes on the mitotic or meiotic spindle (Dewar *et al*, 2004). Cohesion is mediated by cohesin complexes (Guacci *et al*, 1997; Michaelis *et al*, 1997; Losada *et al*, 1998) which are thought to connect sister DNAs by embracing them as rings (Haering *et al*, 2008). These are composed of the subunits SMC1, SMC3 and SCC1 (also known as RAD21 and Mcd1), which are bound by a fourth subunit, in human cells either SA1 or SA2 (also called STAG1 and STAG2, respectively). Cohesin also associates with WAPL and PDS5 proteins, which are believed to control opening and closure of the cohesin ring (Losada & Hirano, 2005; Kueng *et al*, 2006; Nasmyth, 2011).

How cohesin entraps sister DNAs is unknown, but the observation that cohesin can normally establish cohesion only during S phase (Uhlmann & Nasmyth, 1998; Tachibana-Konwalski *et al*, 2010) implies that cohesion establishment is coupled to DNA replication. After S phase, cohesin can establish cohesion only in the presence of DNA double-strand breaks, which activate a DNA replication-independent pathway that can generate cohesion *de novo* (Ström *et al*, 2007; Unal *et al*, 2007).

The notion that cohesion establishment is normally coupled to DNA replication is also supported by the observation that inactivation of several replisome components has been found to cause cohesion defects. The replisome is a macromolecular protein complex that moves processively along DNA, unwinds it with the help of the CDC45-MCM-GINS (CMG) replicative DNA helicase into leading and lagging strands and uses these as templates for DNA synthesis,

<sup>1</sup> Research Institute of Molecular Pathology, Vienna, Austria

<sup>2</sup> Max Planck Institute of Molecular Cell Biology and Genetics, Dresden, Germany

<sup>3</sup> Institute of Molecular Biotechnology, Vienna, Austria

<sup>4</sup> European Molecular Biology Laboratory, Heidelberg, Germany

<sup>5</sup> Vienna Biocenter Core Facilities, NGS Facility, Vienna, Austria

\*Corresponding author. Tel: +43 1 79730 3250; E-mail: jan-michael.peters@imp.ac.at

†Present address: The Francis Crick Institute, London, UK

‡Present address: Department of Biochemistry, Stanford University School of Medicine, Stanford, CA, USA

§Present address: Institute of Analytical Chemistry, University of Vienna, Vienna, Austria

¶Present address: The Antibody Lab, Vienna, Austria

††Present address: IGH, CNRS, University of Montpellier, Montpellier, France

catalysed by the DNA polymerases *alpha*, *delta* and *epsilon* (Yeeles et al, 2015, 2017). Replisome movement is driven by MCM2-7, a heterohexameric ATPase complex that represents the core of the replicative helicase (hereafter abbreviated MCM; reviewed in Deegan & Diffley, 2016). Replisome components that also have roles in sister chromatid cohesion include WDHD1 (also called Ctf4 and AND1), which connects MCM and DNA polymerase *alpha*, the regulatory protein claspin, the DNA helicase CHL1 (DDX11), the endonuclease FEN1, the replication fork-stabilizing timeless–tipin complex (Tof1, Csm3) and the CTF18 subunit of replication factor C (RFC), which loads the DNA polymerase *delta* processivity factor PCNA onto DNA (Hanna et al, 2001; Mayer et al, 2004; Petronczki et al, 2004; Ansbach et al, 2008; Errico et al, 2009; Terret et al, 2009; Borges et al, 2013; Samora et al, 2016). The finding that these replisome-associated proteins have roles in DNA replication and cohesion implies that cohesion establishment may occur directly at or in the vicinity of replication forks from which the newly synthesized sister DNAs emerge.

Cohesion also depends on acetylation of the cohesin subunit SMC3 (Ben-Shahar et al, 2008; Unal et al, 2008; Zhang et al, 2008; Rowland et al, 2009) by members of the Eco1 acetyltransferase family (Skibbens et al, 1999; Tóth et al, 1999; Ivanov et al, 2002; Williams et al, 2003; Hou & Zou, 2005). These modifications have to be generated during DNA replication to support cohesion (Skibbens et al, 1999; Tóth et al, 1999; Song et al, 2012), only affect cohesin on chromatin (Ben-Shahar et al, 2008; Unal et al, 2008) and stabilize cohesin on DNA so it can maintain cohesion until the subsequent mitosis (Gerlich et al, 2006; Ladurner et al, 2016). In vertebrates, SMC3 acetylation enables cohesin to interact with sororin (Lafont et al, 2010; Nishiyama et al, 2010), a protein that is essential for maintaining cohesion from S phase until mitosis (Rankin et al, 2005; Schmitz et al, 2007; Ladurner et al, 2016). Sororin mediates this function by antagonizing WAPL (Nishiyama et al, 2010), which otherwise releases cohesin from DNA precociously (Gandhi et al, 2006; Kueng et al, 2006; Tedeschi et al, 2013). Eco1 also antagonizes Wapl and its binding partner Pds5 in plants (De et al, 2014) and yeasts (Tanaka et al, 2001; Ben-Shahar et al, 2008; Unal et al, 2008; Sutani et al, 2009; Feytout et al, 2011; Chan et al, 2012; Guacci et al, 2015; Beckouët et al, 2016), even though sororin is not known to exist in these organisms. Cohesin acetylation may therefore be essential for stabilizing cohesive cohesin complexes on chromatin and maintaining cohesion in many species. However, in several simple eukaryotic genomes, genes encoding Eco1 orthologs could not be identified (Nasmyth & Schleiffer, 2004; Peters & Nishiyama, 2012), indicating that in some species cohesin acetylation may either be absent or be catalysed by other acetyltransferases. As an additional function, it has been proposed that cohesin acetylation increases the rate of replication fork movement (Terret et al, 2009).

Vertebrate cells contain two Eco1 orthologs called ESCO1 and ESCO2 (also known as EFO1 and EFO2), which differ in their N-terminal sequences but possess highly conserved C-terminal acetyltransferase domains (Hou & Zou, 2005). Whereas ESCO1 is present in quiescent and proliferating cells, ESCO2 is only present in proliferating cells where it is most abundant during S phase (Whelan et al, 2012a). ESCO2 deficiency is the cause of Roberts syndrome (Schüle et al, 2005; Vega et al, 2005), a severe

developmental disorder that often leads to pre-natal or early post-natal death. Prometaphase chromosomes of RBS cells lack the primary constriction that is normally seen in pericentric heterochromatin, leading to a characteristic “railroad” appearance (German, 1979; Tomkins et al, 1979; Louie & German, 1981; Maserati et al, 1991; Van Den Berg & Francke, 1993). This morphology is thought to be caused by defects in centromeric cohesion and can be restored by ectopic expression of ESCO2 (van der Lelij et al, 2009). Cohesion between sister chromatid arms is maintained in RBS cells, presumably due to the presence of ESCO1. The notion that there is partial redundancy between the functions of ESCO1 and ESCO2 is also supported by the observation that SMC3 acetylation and stable cohesin association with chromatin in G2 phase depend on both ESCO1 and ESCO2 (Nishiyama et al, 2010; Ladurner et al, 2016). However, the severity of clinical symptoms observed in RBS patients implies that ESCO2 is essential for development despite its partial redundancy with ESCO1. This conclusion is further supported by the observation that ESCO2 is essential for centromeric cohesion and embryonic development in mice (Whelan et al, 2012b).

How cohesin and its acetyltransferases interact with the replisome to enable establishment and maintenance of cohesion is poorly understood. In yeast, Eco1 interacts with PCNA (Moldovan et al, 2006), has been detected at replication forks (Lengronne et al, 2006) and mediates Smc3 acetylation in a manner that is facilitated by several replisome components (Borges et al, 2013), raising the possibility that Eco1 travels with replication forks to acetylate cohesin in their vicinity. These reactions might be promoted by direct interactions between the replisome component Chl1 and cohesin (Samora et al, 2016). After DNA replication, Eco1 is inactivated by ubiquitin-dependent proteolysis (Lyons & Morgan, 2011; Lyons et al, 2013), but can be reactivated by DNA damage to contribute to *de novo* cohesion establishment (Ström et al, 2007; Unal et al, 2007; Heidinger-Pauli et al, 2009).

In *Xenopus* egg extracts, recruitment of ESCO2 to chromatin and cohesin acetylation depends on pre-replicative complexes (pre-RCs), the inactive precursors of replisomes (Higashi et al, 2012). Human ESCO2 has also been reported to interact with PCNA (Moldovan et al, 2006) and human cohesin with MCM (Guillou et al, 2010), but the functional relevance of these interactions is not known. In contrast, ESCO1 is not known to interact with the replication machinery but has been found to interact with chromatin via cohesin and its PDS5 subunits (Minamino et al, 2015), and is enriched at cohesin binding sites in the genome (Rahman et al, 2015).

To obtain further insight into the roles of DNA replication proteins in establishment and maintenance of cohesion, we isolated 55 proteins implicated in these processes from HeLa cells synchronized in S phase and analysed their interaction partners. This revealed that ESCO2 is associated in near-stoichiometric amounts with MCM on chromatin of replicating cells. Our results indicate that this interaction is required for proper recruitment of ESCO2 to chromatin, cohesin acetylation during DNA replication and centromeric cohesion. We propose that MCM binding enables ESCO2 to travel with replicating replisomes to acetylate cohesive cohesin complexes in the vicinity of replication forks.

## Results

### A proteomic screen to identify interactions between DNA replication and cohesion proteins

To obtain insight into how sister chromatids become stably connected during DNA synthesis (S) phase, we searched for physical interactions between DNA replication proteins and proteins required for cohesion establishment and maintenance. For this purpose, we isolated 55 proteins previously implicated in these processes (Appendix Table S1) from HeLa cells and identified co-purifying proteins by mass spectrometry (MS), using the experimental scheme outlined in Fig 1A. To facilitate protein purification, we tagged the genes encoding these proteins on bacterial artificial chromosomes (BACs) by using high-throughput recombineering technology developed by the MitoCheck consortium (Poser *et al*, 2008; Hutchins *et al*, 2010) and stably expressed these BACs in HeLa cell pools. The “BAC TransgeneOmics” technique allows the expression of tagged genes under their own promoters at near physiological levels (Poser *et al*, 2008). In most cases, mouse genes were tagged (Appendix Table S1) because these can usually replace their human orthologs but offer the advantage that the functionality of the tagged proteins can be tested by RNA interference (RNAi)-mediated depletion of the endogenous human counterparts (Poser *et al*, 2008). We use standard nomenclature to distinguish between mouse and human proteins (for example, *Esco2* and *ESCO2*, respectively), but use the human acronym when summarizing results obtained with orthologs from both species.

Proteins were tagged with a combined localization and affinity purification (LAP) tag (Cheeseman & Desai, 2005; Poser *et al*, 2008; Fig 1B) and isolated by single-step immunoprecipitation with antibodies directed against the green fluorescent protein (GFP) moiety of the LAP tag. To identify protein interactions that might occur during cohesion establishment, cells were arrested at the G1-S phase transition by a single thymidine treatment and released for 2.5 h into mid-S phase. Proteins were purified either from whole-cell lysates, or from fractions containing soluble or chromatin-bound proteins, and analysed by in-solution trypsinization and tandem MS, and separately by sodium dodecyl sulphate–gel electrophoresis (SDS–PAGE) and silver staining (for examples, see Fig 1C; the interactions and a summary of each experiment are available on [www.mitocheck.org](http://www.mitocheck.org)).

When we analysed reciprocal interactions, i.e. those that were detected between two proteins that had both been used as “baits”, we identified four discrete clusters of interacting proteins in samples isolated from whole-cell lysates. These corresponded to cohesin, the cohesin loading complex (NIPBL-MAU2), the origin recognition complex (ORC) and a cluster containing other replication proteins, including RFC subunits, the timeless–tipin complex, MCM and the GINS complex (Fig 1D). In this data set, cohesin and the cohesin loading complex did not reciprocally interact with replication proteins. However, the cohesin acetyltransferase *ESCO2* did reciprocally interact with five of the six subunits of MCM (Fig 1D). Samples obtained by *Esco2*-LAP isolation from whole-cell lysates also contained other DNA replication proteins and cohesin, which were detected as “bait–prey” interactions, i.e. not reciprocally. Furthermore, when rank-ordered according to sequence coverage or peptide spectrum matches (PSMs; the number of tandem mass spectra that match peptides from a particular protein), all six MCM subunits scored highest, indicating that *ESCO2* interacts predominantly

with this complex (Fig 2A; see also Fig EV1C). In all subsequent experiments reported here, we therefore further characterized *ESCO2*-MCM interactions.

To analyse all interactions between cohesion and replication proteins systematically, we mapped the proteins to Ensembl v82. This identified in total 84 such interactions, 72 of which were only detected non-reciprocally, and 19 of which were previously reported (Kenna & Skibbens, 2003; Guillou *et al*, 2010; Leman *et al*, 2010; Panigrahi *et al*, 2012). These interactions are listed in Appendix Table S2 as a resource for further studies.

### *ESCO2* interacts with the MCM replicative helicase on chromatin

*ESCO2*-MCM interactions could only be detected when *Esco2* (Fig 2B) or *Mcm2*, *Mcm4*, *Mcm5*, *Mcm6* and *Mcm7* (Fig 2C) were purified from samples containing chromatin proteins, but not from soluble fractions, indicating that *ESCO2*-MCM interactions occur predominantly on chromatin (note that the whole-cell extracts in which *ESCO2*-MCM interactions were originally detected were prepared with the addition of nucleases, resulting in the presence of both soluble and chromatin proteins). In contrast, *Mcm3*-LAP could only be purified from soluble fractions in which it was not associated with *ESCO2* (Fig 2C). Because the evolutionarily conserved C-terminal domain of budding yeast *Mcm3* is essential for loading of MCM onto chromatin (Frigola *et al*, 2013), the LAP tag fused to the C terminus of *Mcm3* may have inhibited the loading of the respective MCM complexes onto chromatin in our experiments and may thus have prevented their association with *ESCO2*. Analysis of all reciprocal bait–bait interactions detected in our MS dataset confirmed that *ESCO2* specifically interacts with MCM on chromatin but not in soluble fractions (Fig EV1A–C).

At lower levels, the *Esco2*-LAP samples also contained proteins that only associate with MCM during helicase activation and are required for this process (Leman & Noguchi, 2013; Siddiqui *et al*, 2013; Fragkos *et al*, 2015), such as MCM10, *treslin*, *CDC45*, *GINS3*, *GINS4* and *DDK* (*CDC7* and *DBF4*), and proteins required for replisome progression such as *RFC* (Figs 2A, and EV1B and C). This implies that *ESCO2* associates with MCM as part of pre-RCs and remains associated with the replicative helicase during DNA synthesis (for experimental tests of this hypothesis, see Fig 9 below).

To obtain insight into how *ESCO2* binds to MCM, we used amine-reactive chemical cross-linking-MS (CLMS) to obtain a lysine proximity map of *ESCO2*-MCM complexes. For this purpose, we immunoprecipitated *ESCO2* and the associated MCM from chromatin fractions obtained from two different sources. In one case, we used fibroblasts derived from *ESCO2*-deficient RBS patients in which we had ectopically expressed GFP-*ESCO2* from a cDNA. The defects in centromeric sister chromatid cohesion that are observed in these cells are restored by GFP-*ESCO2* expression (see Fig 7 below; van der Lelij *et al*, 2009), demonstrating that GFP-*ESCO2* is functional. In the other case, we used the BAC transgenic HeLa cells expressing mouse *Esco2*-LAP originally used in the proteomic screen. Proteins from both sources were treated with bisulphosuccinimidyl suberate (BS3) or disuccinimidyl suberate (DSS; both spanning 11.4 Å), and the extent of cross-linking was analysed by SDS–PAGE and silver staining (Fig 2D). Cross-linked tryptic peptides identified in these samples by MS are listed in Appendix Table S3. Of 33 cross-links that we detected between MCM subunits, 29 (88%) connected

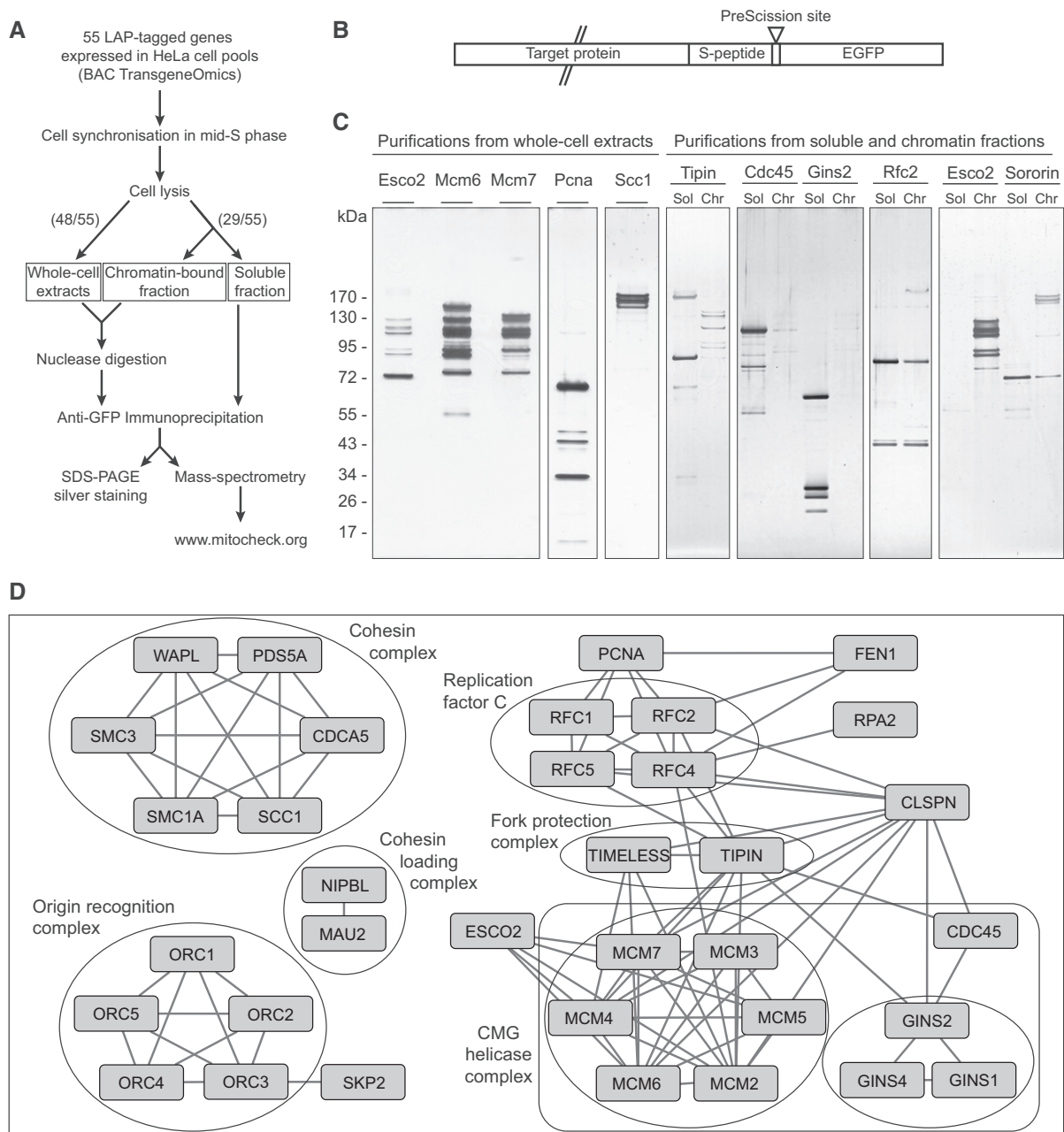


**Figure 1. A candidate proteomic screen identifies novel interactions between cohesin factors and the replisome.**

**A** Schematic outline of the LAP-tag purification mass spectrometry procedure. Out of 55 LAP-tagged proteins, 48 were purified from whole-cell extracts and 29 from soluble and chromatin-bound fractions. All resulting MS data can be viewed at [www.mitocheck.org](http://www.mitocheck.org).  
**B** Schematic depiction of a bait protein fused at its C terminus to the 30-kDa LAP tag. The LAP tag comprises a S-peptide binding site, a PreScission protease cleavage site and EGFP. Not drawn to scale.  
**C** Examples of complexes purified via the indicated bait proteins from whole-cell extracts or soluble (Sol) and chromatin-bound (Chr) fractions, analysed by SDS-PAGE and silver staining.  
**D** Reciprocal bait-bait interactions identified among the proteins purified from whole-cell extracts. For related analyses, see Fig EV1A and B.

neighbouring subunits (visualized as Circos diagrams in Fig EV1D). This indicates that our CLMS conditions enabled the identification of specific protein interactions. Between ESCO2 and MCM, we identified in total 36 cross-links, 20 on human ESCO2 and 16 on mouse Esco2 (Fig 2E and F). On MCM, 26 (72%) of these cross-links were

located on MCM4 and MCM7, which are neighbouring subunits in the helicase complex (Fig EV1E and F). On ESCO2, 32 (89%) of the cross-links to MCM were located in the N-terminal 235 residues. These results indicate that the N terminus of ESCO2 associates with the replicative helicase by binding to MCM4 and MCM7.

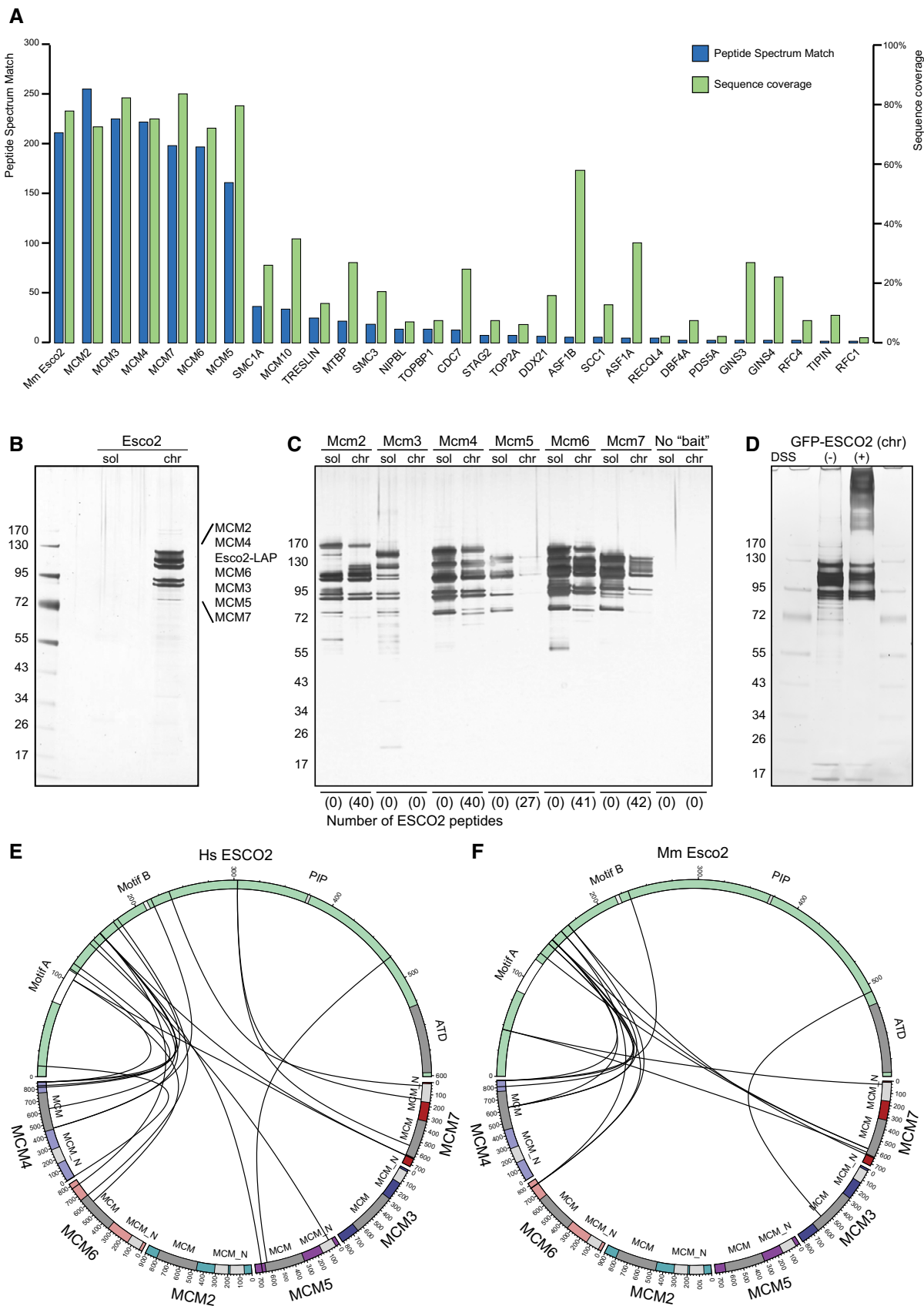


Figure 2.

**Figure 2. ESCO2 interacts with the MCM replicative helicase on chromatin.**

- A A plot of peptide spectrum matches (blue, left axis) and percentage sequence coverages (green, right axis) of proteins identified by MS in EscO2-LAP samples purified from whole-cell extracts.
- B Purified EscO2-LAP samples from soluble and chromatin-bound fractions, analysed by SDS-PAGE and silver staining. Note that MCM co-immunoprecipitates with EscO2-LAP from chromatin but not soluble fractions (see also Fig EV1C).
- C MCM purified from soluble and chromatin fractions, analysed by SDS-PAGE and silver staining. The number of ESCO2 peptides identified in each immunoprecipitate is indicated in parentheses.
- D GFP-ESCO2 samples purified from chromatin, analysed by SDS-PAGE and silver staining before and after treatment with DSS.
- E Circos plot representing identified cross-links between human ESCO2 and MCM. Note that ESCO2 is not drawn to scale relative to MCM subunits. The positions of the A, B, and PIP motifs in ESCO2 are depicted in white. The ESCO2 acetyltransferase domain, the MCM domains and MCM-N-terminal domains are depicted in grey.
- F Circos plot representing identified cross-links between mouse EscO2 and MCM. Note that EscO2 is not drawn to scale relative to MCM subunits.

**ESCO2-chromatin interactions become more dynamic in G2 phase, concomitant with dissociation of MCM from chromatin**

The observation that ESCO2 associates with MCM on chromatin during S phase raised the possibility that this interaction might facilitate cohesin acetylation at replication forks. We therefore analysed whether ESCO2-MCM interactions are required to recruit ESCO2 to chromatin and to mediate cohesion. We were unable to fully deplete MCM by RNA interference and could thus not test directly if the replicative helicase is needed for ESCO2's chromatin association. However, MCM is known to dissociate from chromatin in G2 phase (Kuipers *et al*, 2011). We therefore analysed whether ESCO2-chromatin interactions are different in S phase and G2. For this purpose, we measured the chromatin association of GFP-ESCO2 by fluorescence recovery after photobleaching (FRAP) in RBS cells that had been synchronized by aphidicolin arrest in early S phase or by release from this arrest in mid-S phase or in G2 phase (Fig 3A and B). In these experiments, we observed slower recovery of GFP-ESCO2 from photobleaching in cells synchronized in early and mid-S phase than in cells in G2 (Fig 3C and D), concomitant with the dissociation of MCM from chromatin (Fig 3B). Curve fitting indicated the existence of two GFP-ESCO2 populations with different dwell times, a "fast" population with a half-life of 2–4 s, a "slow" population with a mean residence time of more than 1 min under aphidicolin arrest and in mid-S phase, and less than half a minute in late S-G2 phase (Fig 3E and F). We assume that these two populations represent ESCO2 molecules that interact with chromatin only very transiently or not at all, and chromatin-bound ESCO2, respectively. Importantly, both the relative abundance and the residence time of the "slow" population declined as cells proceeded to G2 phase (Fig 3E and F; note that the 7.5 h release time point contains "outliers" with longer residence times similar to the ones seen in S phase, implying that these particular cells had not completed DNA replication, consistent with the FACS profile in Fig 3A; it is therefore possible that in G2 phase, the dwell time of the putative slow ESCO2 population is comparable to non-chromatin-bound ESCO2). These results are consistent with the hypothesis that MCM mediates stable recruitment of ESCO2 to chromatin.

**ESCO2's PBM-A motif is required for binding to MCM**

To test this hypothesis more directly and to be able to analyse whether ESCO2-MCM interactions are required for cohesion, we searched for ESCO2 mutants that are defective in MCM binding. Interestingly, the MCM-interacting region that we had identified in ESCO2 (10–235) contains two motifs, called PBM-A and PBM-B, that are required for chromatin association of ESCO2 in *Xenopus* egg

extracts (Higashi *et al*, 2012). Because this interaction depends on pre-RCs, of which MCM is a component, we hypothesized that ESCO2 might bind to MCM via PBM-A or PBM-B. These regions (in most figures called A and B for brevity) are evolutionarily more conserved than the rest of ESCO2's sequences (except for the acetyltransferase domain, which is also highly conserved; Fig 4A; Higashi *et al*, 2012) and are predicted to be ordered, whereas most other N-terminal sequences are predicted to be disordered (Fig 4A). We therefore generated ESCO2 mutants lacking PBM-A (residues 75–110;  $\Delta A$ ) or PBM-B (residues 208–212;  $\Delta B$ ) or both ( $\Delta AB$ ). In addition, we created ESCO2 mutants in a PIP box (Q374A, I376A, I377A; PIP<sup>mut</sup>), a sequence that in several other proteins mediates binding to PCNA (Warbrick, 1998). All ESCO2 mutants characterized in this study and a summary of their properties are shown schematically in Fig 4B.

To test whether these mutants can associate with MCM, we stably expressed them as N-terminally GFP-tagged proteins from cDNAs in RBS immortalized fibroblasts and purified them via their GFP tags from cells synchronized in S phase (Appendix Fig S1). Interestingly, this revealed that ESCO2 versions with PBM-B deletion or PIP box mutation were still able to bind MCM, whereas three different mutants that were lacking PBM-A were not (Fig 5A). Label-free quantitative MS, performed with three independently purified samples for wild-type ESCO2 and each mutant, confirmed that deletion of PBM-A resulted in a dramatic reduction of MCM when compared to wild-type GFP-ESCO2 or mutants only mutated in PBM-B or the PIP box (Figs 5B, upper panels, and EV2; Dataset EV1). Conversely, deletion of PBM-B correlated with an under-representation of the cohesin subunits SMC1, SMC3, SA2 and SCC1 (Fig 5B, lower panels). These differences were not due to defects in cellular localization or cell cycle-dependent fluctuations in protein levels, as time-lapse microscopy experiments revealed that all mutants accumulated in nuclei at the time predicted for S phase (Appendix Fig S2, Movies EV1–EV5), as does wild-type ESCO2 (van der Lelij *et al*, 2009); note that we also detected GFP-ESCO2 in nucleoli, as did van der Lelij *et al*, 2009, although the functional relevance of this localization is unknown). These results indicate that ESCO2's PBM-A motif is essential for MCM binding, whereas PBM-B might contribute to interactions with cohesin.

**ESCO2 mutants deficient in MCM binding cannot stably associate with chromatin**

To test whether MCM binding is required for recruitment of ESCO2 to chromatin, we analysed the ESCO2 mutants described above in four different assays. First, we analysed soluble and chromatin

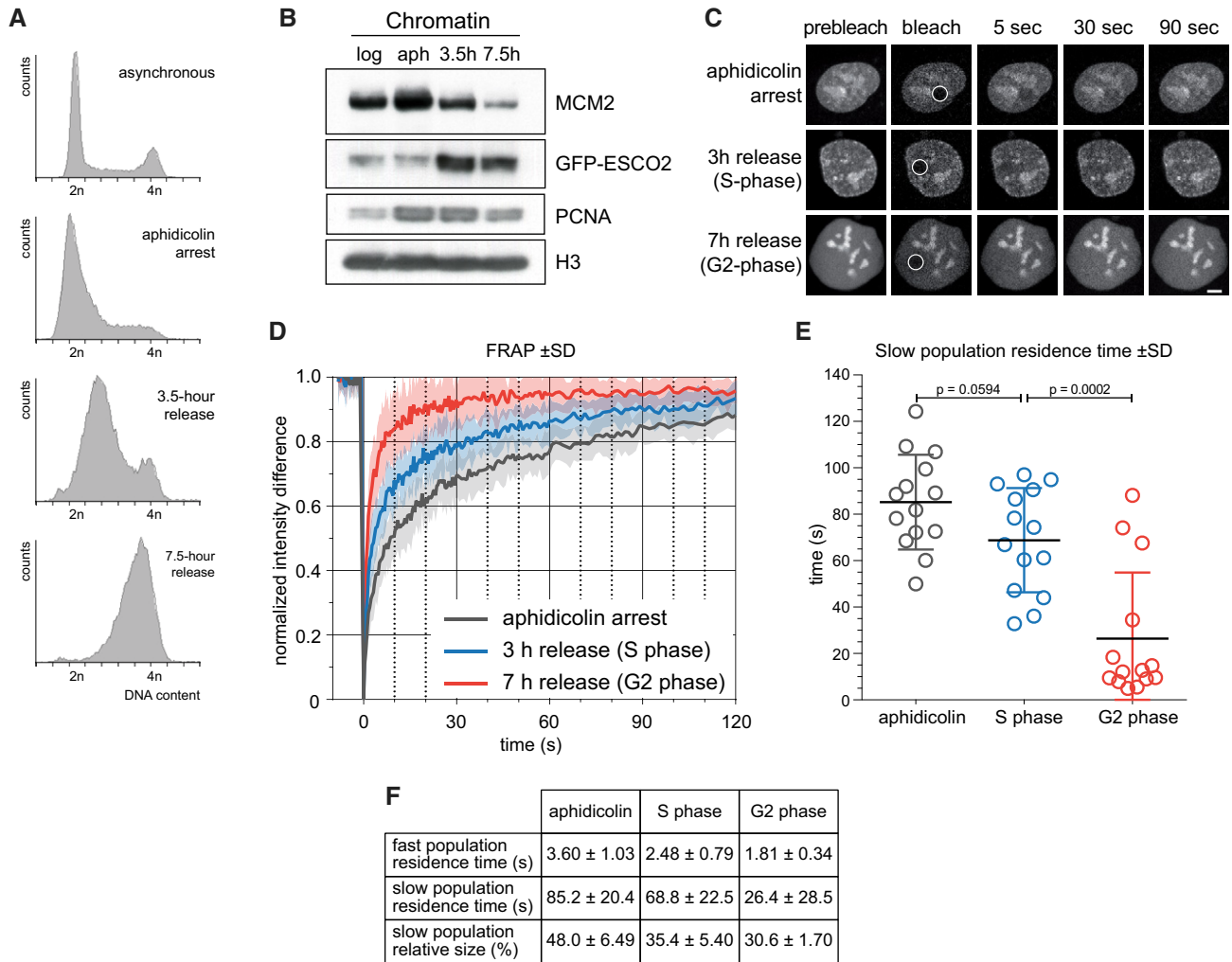


**Figure 3. The association of ESCO2 with chromatin becomes more dynamic after DNA replication concomitant with MCM dissociation.**

**A** DNA content distribution of asynchronous or cell cycle-synchronized RBS cells expressing GFP-ESCO2, as measured by propidium iodide staining and FACS.  
**B** Immunoblot analysis of chromatin-bound proteins showing dissociation of MCM2 from chromatin during DNA replication. Note that ESCO2 associated maximally with chromatin during S phase.  
**C** Still images of fluorescence recovery measured by FRAP. RBS cells expressing wild-type GFP-ESCO2 were arrested in S phase by aphidicolin treatment, or aphidicolin-arrested and then released for 3 h (mid-S) or 7 h (late S/G2). White circles represent sites of bleaching (2  $\mu$ m radius). Scale bar, 5  $\mu$ m.  
**D** Average FRAP profiles of normalized fluorescent signals  $\pm$  standard deviation (SD) from cells treated as in (C). Bi-exponential curve fitting indicates the presence of a fast and a slow ESCO2 population.  $n = 14$  cells per condition.  
**E** Mean residence time of chromatin-bound GFP-ESCO2 calculated from (D). Error bars denote SD. Significance levels were quantified by unpaired t-test.  
**F** Quantification of the residence times and the relative abundance ( $\pm$  SD) of the fast and slow populations of GFP-ESCO2.

fractions from S phase synchronized cells expressing the ESCO2 mutants by immunoblotting (Fig EV3A). While all variants could be detected in chromatin fractions under these conditions, more ESCO2 was present in the soluble fraction relative to the chromatin fraction when PBM-A was deleted, but not when PBM-B was deleted or the PIP box mutated.

Second, we analysed the localization of ESCO2 mutants by confocal microscopy in living RBS cells in which replication foci were labelled by expression of RFP-PCNA (Appendix Fig S3A). For wild-type,  $\Delta$ B and PIP box mutated GFP-ESCO2, we observed a punctate pattern during S phase (as judged by the presence of PCNA foci), similar in appearance to replication foci, whereas mutants in which

PBM-A had been deleted showed a more homogeneous distribution. Interestingly, we noticed that GFP-ESCO2 and RFP-PCNA foci were often located next to each other but did not overlap, reminiscent of the localization of MCM and PCNA, which are also located adjacent to each other in S phase (Dimitrova *et al*, 1999; Brand *et al*, 2007; Kuipers *et al*, 2011). For technical reasons, we were unable to directly co-localize ESCO2 and MCM, but the observation that both of them are located next to PCNA in S phase is consistent with the possibility that ESCO2 and MCM co-localize during this cell cycle phase. In contrast, all GFP-ESCO2 mutants were homogeneously distributed in nuclei in cells lacking replication foci, i.e. those that had presumably reached G2 phase (Appendix Fig S3B).

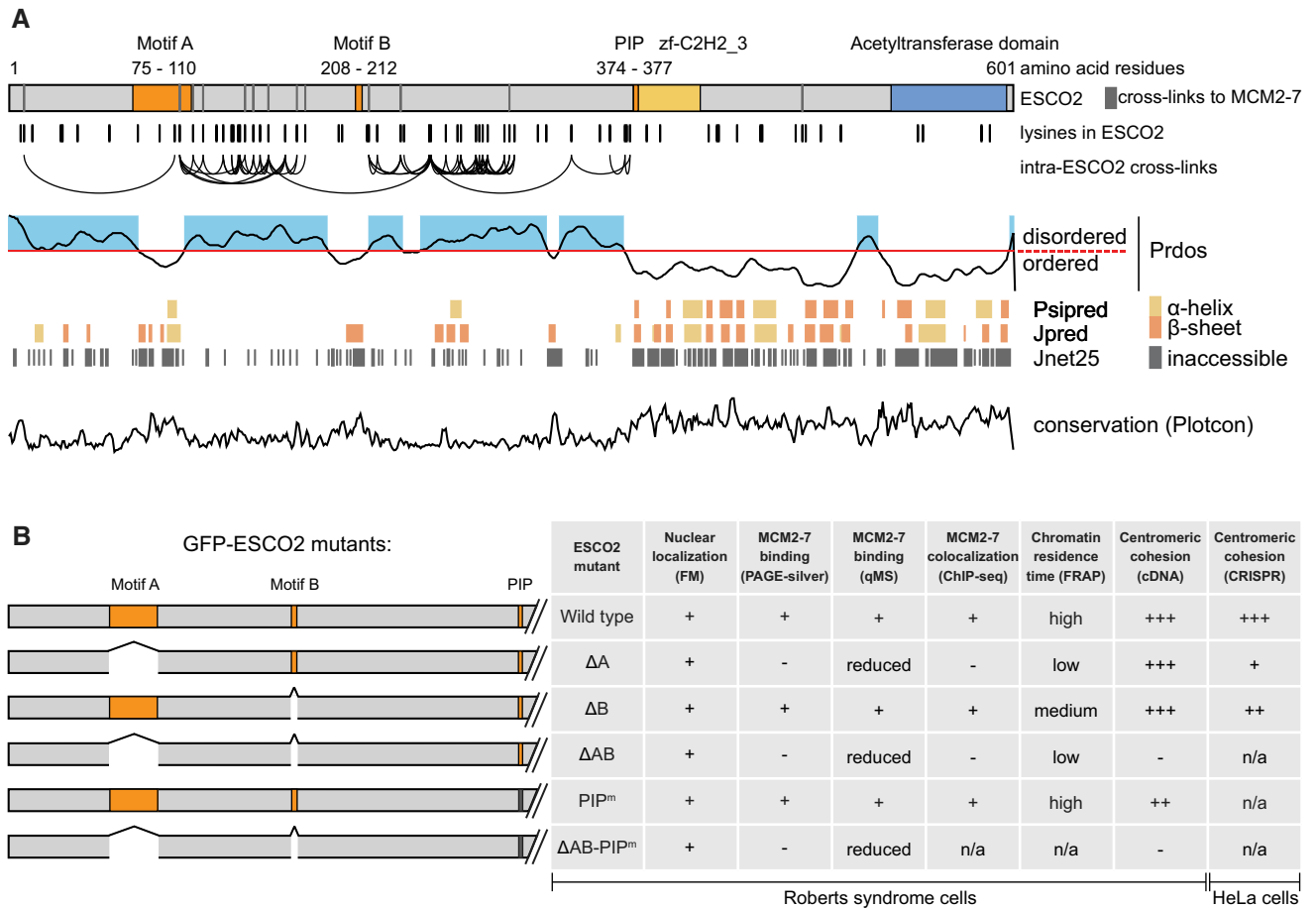


**Figure 4. Conserved ESCO2 motifs confer distinct functional interactions.**

**A** Top to bottom: Schematic representation of human ESCO2 denoting the positions of PBM-A (motif A) and PBM-B (motif B), PIP box, Zn-finger domain and acetyltransferase domain; positions of cross-links to MCM subunits (grey bars); positions of all other lysine residues in ESCO2 (black bars); intra-ESCO2 cross-links generated by DSS and BS3; disordered regions predicted using PrDOS (Ishida & Kinoshita, 2007); secondary structure predictions made by PISPRED (Jones, 1999) and Jpred (Drozdetskiy *et al.*, 2015); residues classified as buried by Jnet using a 25% relative solvent accessibility cut-off (in grey); evolutionary conservation among vertebrates calculated and plotted using EMBOSS plotcon with a window size of three residues.

**B** Schematic representation of N-terminally GFP-tagged human ESCO2 mutants and a summary of their intracellular localization (fluorescence microscopy, FM), ability to bind MCM (IP-SDS-PAGE-silver staining and label-free qMS), co-localization with MCM3 on chromatin (ChIP), chromatin-bound residence time (FRAP) and ability to restore centromeric sister chromatid cohesion (chromosome spreads) when expressed from cDNAs in RBS cells or when endogenously modified by CRISPR-Cas9 in HeLa cells. Number of (+) in the last two columns indicates relative strength of centromeric cohesion. n/a - no such experiments have been performed.

Third, we performed FRAP assays as in Fig 3C by bleaching a circular spot of nuclear GFP-ESCO2 in S phase cells. In this assay, mutation of the PIP box had no effect whereas deletion of PBM-A or PBM-B reduced chromatin residence times significantly, with the effect of PBM-A deletion being much stronger than the effect of PBM-B deletion (Fig 6A–D). Notably, the residence time of ESCO2- $\Delta A$  was similarly short (12.5–16.5 s, Fig 6D) as the residence time of wild-type ESCO2 in G2 phase (26 s; Fig 3F), indicating that this mutant can interact with chromatin only very transiently. The residence time of ESCO2- $\Delta AB$  was slightly but not significantly shorter than that of ESCO2- $\Delta A$ , indicating that in human cells, ESCO2-chromatin interactions depend mainly on PBM-A. Similar results were obtained with fast-acquisition FRAP experiments (Fig EV3B and C).

Fourth, we used chromatin immunoprecipitation (ChIP) followed by next-generation Illumina sequencing (ChIP-seq) to compare the genomic distribution of wild-type and mutated ESCO2 to the

distribution of MCM (analysed with MCM3 antibodies) in cells synchronized by aphidicolin arrest. Both MCM3 and ESCO2 ChIP-seq signals were broadly distributed throughout the genome, without clear enrichment in well-defined binding “peaks” (Fig 6E and F), possibly reflecting the well-known abundant presence of MCM on chromatin (Das *et al.*, 2014) and/or variable distributions of MCM and ESCO2 in different individual cells. However, the ChIP-seq patterns of wild-type ESCO2 and MCM3 were remarkably similar. This was also true for ESCO2  $\Delta B$  or  $PIP^m$ , but not for mutants lacking PBM-A. The difference in genomic binding patterns between ESCO2 mutants lacking PBM-A vs. the other forms of ESCO2 (wild-type,  $\Delta B$ ,  $PIP^m$ ) and MCM was also evident in some early replicating regions such as the c-myc origin (Lucas *et al.*, 2007). These were largely devoid of MCM (Fig 6F), possibly because some DNA replication is known to occur even in the presence of aphidicolin (Kaufman *et al.*, 2007). Interestingly, the forms of ESCO2 that



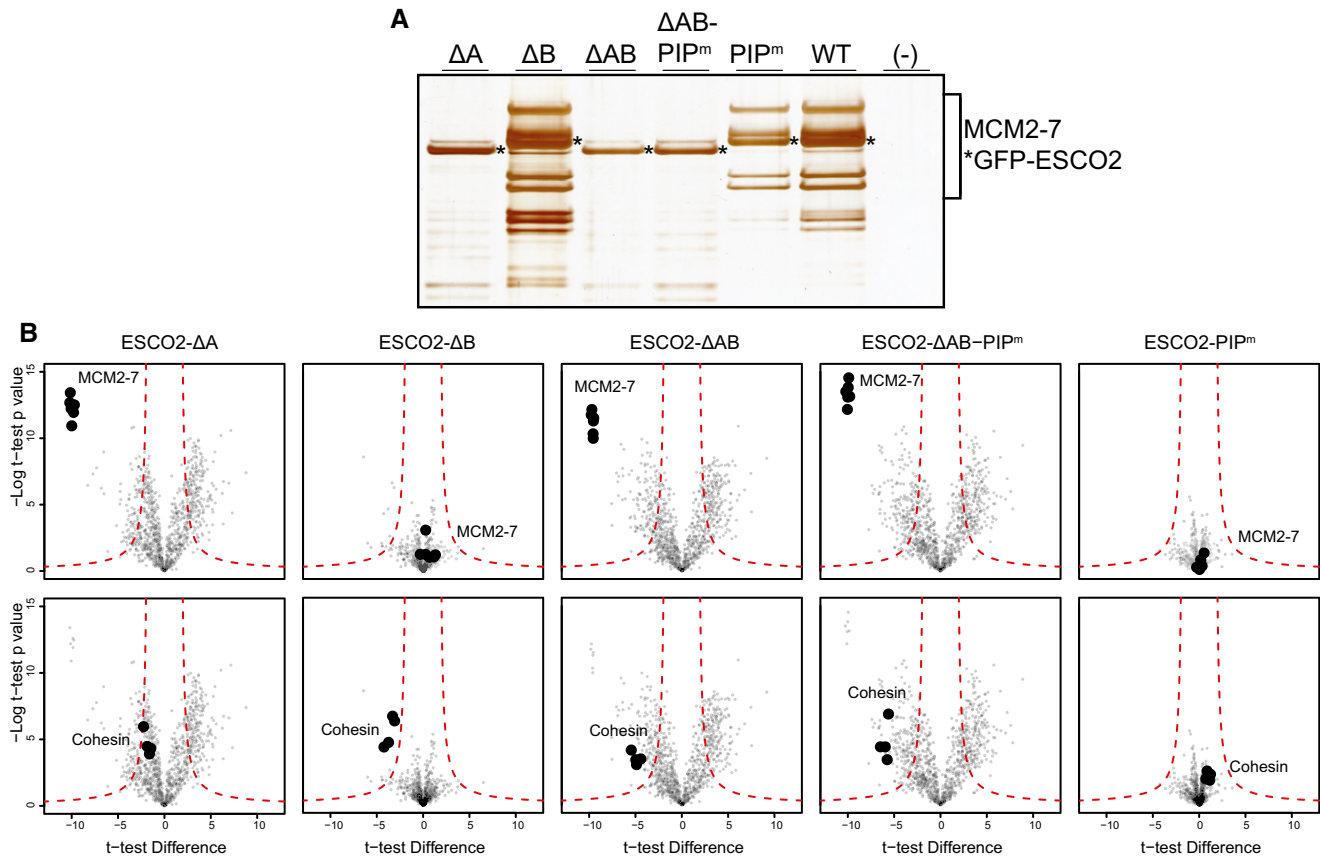


**Figure 5. ESCO2 motif A is required for binding to MCM and motif B facilitates interaction with cohesin.**

A GFP immunoprecipitates isolated from RBS cells that stably expressed wild-type or mutant forms of GFP-ESCO2, analysed by SDS-PAGE and silver staining. Cells were enriched in S phase by aphidicolin arrest followed by a 3-h release. Non-transfected RBS cells were used as a negative control (-).

B Volcano plots of label-free qMS data, representing the abundance of interacting proteins in immunoprecipitates of GFP-tagged ESCO2 mutants relative to wild-type GFP-ESCO2. Area above and to the left of the red dashed line denotes significantly under-represented proteins. Upper panels highlight the abundance of the six MCM subunits. Lower panels highlight the abundance of the cohesin subunits SMC1, SMC3, SCC1 and SA2. For further details, see Fig EV2. Analysis is based on biological triplicates, each subjected to a technical triplicate.

are able to bind to MCM (wild-type,  $\Delta B$ ,  $PIP^m$ ) were also reduced in these regions. In contrast, ESCO2 mutants defective in MCM binding showed different patterns and were not “cleared” from these regions. The fact that the mutants defective in MCM binding could be detected on chromatin by ChIP-seq at all may reflect weak or transient interactions which could also be detected by FRAP (Fig 6A–D; note that our non-calibrated ChIP-seq data do not allow a direct comparison of the amounts of the various forms of ESCO2 on chromatin). To compare these patterns genomewidely, we identified sites enriched in ChIP-seq reads by the BayesPeak algorithm (Spyrou *et al*, 2009) with 1,000 base pair bins and determined the co-occurrence of ESCO2 and MCM3 signals with IntervalStats (Chikina & Troyanskaya, 2012). This confirmed a high degree of genomewide co-localization between MCM3, wild-type,  $\Delta B$  and  $PIP^m$  versions of ESCO2, but not with the ESCO2 mutants lacking PBM-A (Fig 6G).

In summary, we could demonstrate that the ESCO2 mutants deficient in MCM binding showed defective chromatin interactions or localization patterns. This indicates that the ability of ESCO2 to bind MCM is required for proper recruitment of ESCO2 to chromatin.

### ESCO2 mutants deficient in MCM binding cannot mediate centromeric cohesion if expressed at endogenous levels

To test whether the binding of ESCO2 to MCM is essential for centromeric cohesion, we used two different experimental systems. In one case, we used a “rescue-of-function” approach by analysing if the ESCO2 mutants can restore centromeric cohesion in RBS cells (Fig 7A–C). In the other, we used a “loss-of-function” approach by introducing the same PBM-A and PBM-B deletions into the endogenous ESCO2 alleles of HeLa cells by CRISPR-Cas9-mediated genome editing and analysing whether these mutations would cause centromeric cohesion defects (Fig 7E–H). Compared to the first approach, the latter created the important added value that we could analyse the functions of ESCO2 mutants when these were expressed at endogenous levels. In contrast, we found that ectopic expression from cDNAs resulted in ESCO2 levels above the endogenous ones observed in HeLa cells (Fig 7D), which can lead to overexpression artefacts.

To analyse cohesion, logarithmically proliferating cells were enriched in prometaphase by a short nocodazole arrest, followed by mitotic shake-off, spreading on glass slides and staining of chromosomes with Giemsa. In RBS cells, in which ESCO2 expression from

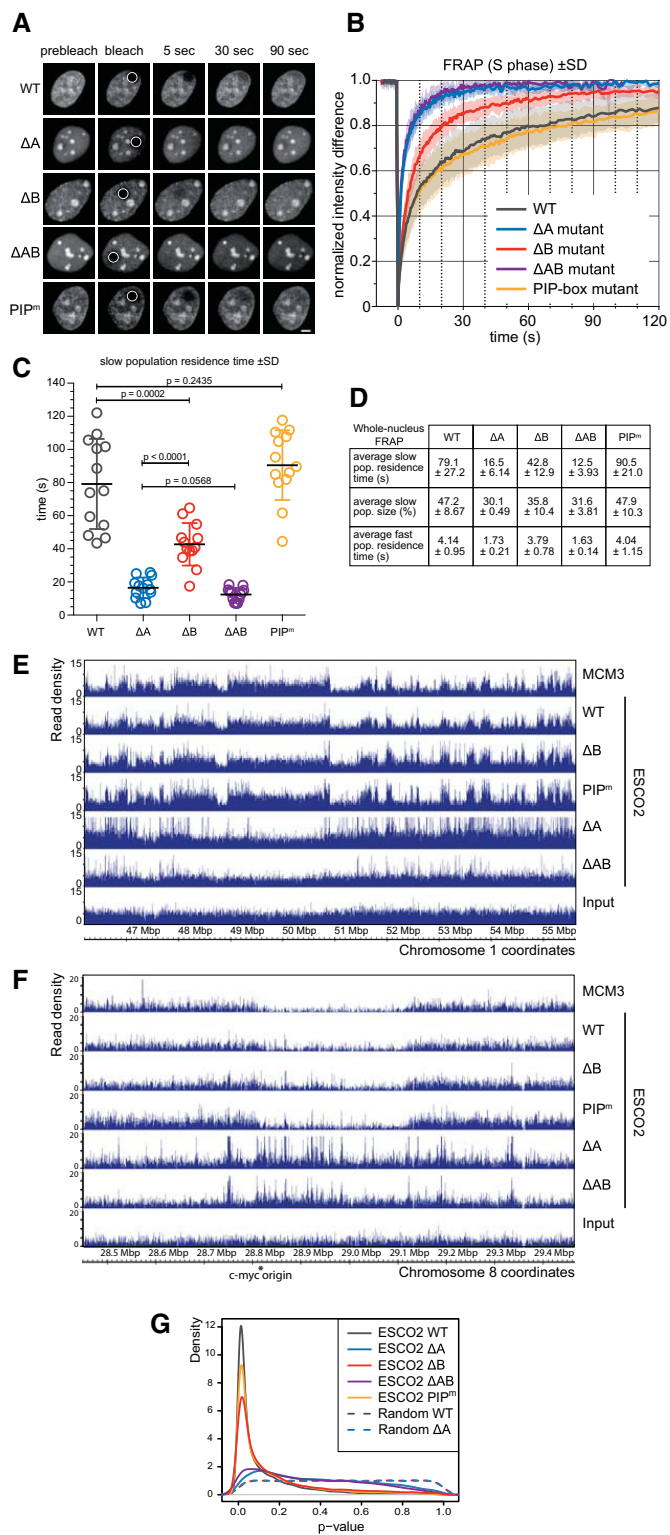


**Figure 6. ESCO2 mutants deficient in MCM binding cannot stably associate with chromatin and do not co-localize with MCM in the genome.**

- A Still images of FRAP experiments of RBS cells expressing wild-type or mutant variants of GFP-ESCO2 and synchronized in S phase by aphidicolin arrest followed by a 3-h release (see also Appendix Figs S1–S3). White circles represent sites of bleaching (2 μm radius). Scale bar, 5 μm.
- B Average FRAP profiles of 13 cells per condition ±SD.
- C Average residence time of ESCO2 variants determined by bi-exponential curve fitting ±SD.
- D Detailed quantification of fast and slow population residence times ±SD and relative abundance.
- E ChIP-seq profiles obtained with MCM3 antibodies and wild-type or mutant GFP-ESCO2 isolated from aphidicolin-arrested (early S phase) RBS cells plotted as chromosome coordinate vs. read density.
- F ChIP-seq profiles as in (E) in the vicinity of the early replicating c-myc origin. Note that partial replication during the arrest locally removes MCM3 and the MCM-interacting ESCO2 variants.
- G IntervalStats P-value distributions of wild-type and mutant GFP-ESCO2 ChIP-seq peaks relative to MCM3 ChIP-seq peaks. P-values close to 0 indicate high co-localization. Homogenous distribution of P-values indicates that peaks are not co-localized, but placed randomly to each other. As controls, the positions of GFP-ESCO2 wild-type and ΔA peaks were randomized before co-localization with MCM3 peaks was examined (dashed lines).

mutants were expressed from endogenous alleles at physiological levels (Fig 7E). In this case, ESCO2 lacking PBM-A enabled centromeric cohesion in many fewer cells (30%) than ESCO2 mutated in PBM-B (60%; Fig 7F and G). We did not create PIP box mutants in these cells as we had found this motif to be dispensable for MCM and chromatin binding. These results indicate that ESCO2 can perform its function with reduced binding to MCM only if ESCO2 is overexpressed, but that at normally occurring ESCO2 levels ESCO2-MCM interactions are important for centromeric cohesion.

Because ESCO2 is thought to contribute to cohesion maintenance by acetylating cohesin on chromatin, we tested whether HeLa cells expressing ESCO2 mutants that are defective in MCM and chromatin interactions contain reduced levels of acetylated SMC3 on chromatin. Immunoblot experiments using an antibody specific for acetylated SMC3 (SMC3(ac); Nishiyama *et al*, 2010) indeed revealed reduced levels of acetylated SMC3 in the mutated cell lines, but only if ESCO1 was depleted by RNAi (Fig 7H). This observation is consistent with the possibility that ESCO2 is required for SMC3 acetylation and cohesion maintenance specifically at centromeres, but not on chromosome arms, where ESCO1 may perform redundant functions.

**ESCO1 and ESCO2 are specifically required for cohesion between chromosome arms and centromeres, respectively**

To test directly whether ESCO1 and ESCO2 perform redundant functions on chromosome arms, we depleted them singly or in combination by RNAi (Fig 8A) and analysed sister chromatid cohesion in mitotic chromosome spreads (Fig 8B and C). As expected, centromeric cohesion was lost in 73% of all ESCO2-depleted cells, but only in 15% of ESCO1-depleted cells. Surprisingly, however, 61% or ESCO1-depleted cells had fully separated chromosome arms, a condition that could only be observed in 20% of control cells. Co-depletion of ESCO1 and ESCO2 resulted in loss of both arm and centromere cohesion in 53% of cells, i.e. in single chromatids.

To test the specificity of the ESCO1 RNAi depletion phenotype, we analysed near-haploid HAP1 cells in which a frameshift mutation had been generated in the ESCO1 gene by gene-trap

cdNAs leads to overexpression, ESCO2 mutants with PBM-A or PBM-B deletions could restore centromeric cohesion in most cells, the PIP box mutant had this effect in only about half of all cells, and only the ESCO2 lacking both PBM-A and PBM-B failed to restore cohesion in almost all cells (Fig 7A and B). Interestingly however, different results were obtained in HeLa cells in which ESCO2

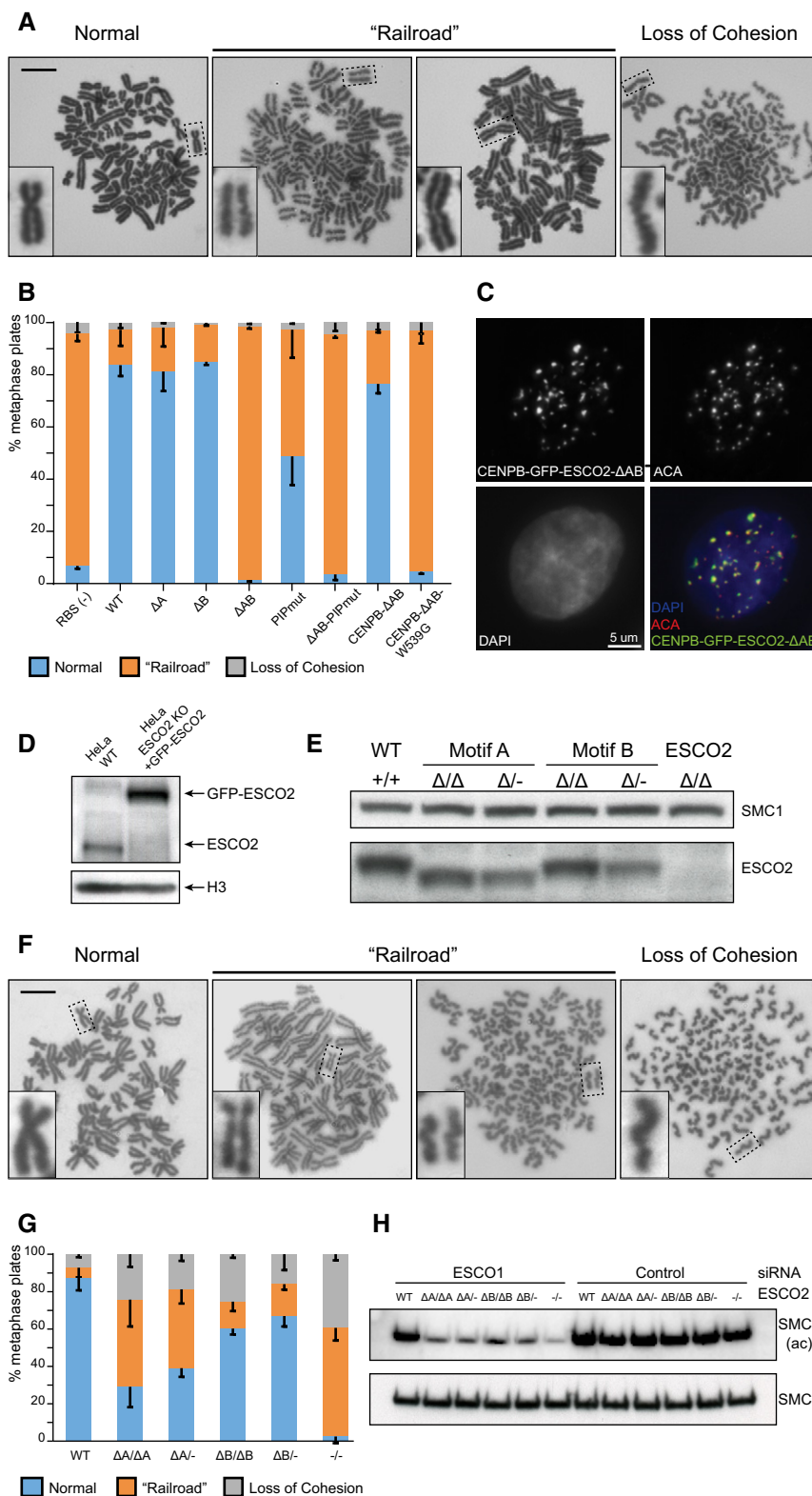


Figure 7.

mutagenesis (Bürckstümmer *et al*, 2013). These cells are viable, even though no ESCO1 protein could be detected in them (Fig 8D). Also in these cells, mitotic chromosome arms were more frequently separated (in 73% of cells) than in HAP1 wild-type cells (38%).

These observations indicate that ESCO1 is not essential for cell viability but has a specific role in mediating proper arm cohesion that ESCO2 cannot fully substitute for, even though ESCO2 can be detected on chromosome arms in ChIP-seq experiments (Fig 6E).

**Figure 7. ESCO2 mutants deficient in MCM binding cannot mediate centromeric cohesion when expressed at endogenous levels.**

- A Representative examples of metaphase chromosome spread from RBS cells. From left to right: normal (wild-type GFP-ESCO2), railroad or loss-of-cohesion phenotypes (non-transfected RBS cells). Scale bar, 10  $\mu\text{m}$ .
- B Metaphase chromosome spread analysis from RBS cells ectopically expressing wild-type or mutant GFP-ESCO2 from cDNA. Error bars represent (–) SD based on two independent blinded experiments, each with  $n \geq 100$ .
- C CENPB<sup>1–160</sup>-GFP-ESCO2- $\Delta$ AB localizes to centromeres. CENPB<sup>1–160</sup>-GFP-ESCO2- $\Delta$ AB and centromeres were visualized using anti-GFP and anti-centromeric antibodies (ACA), respectively. Scale bar, 5  $\mu\text{m}$ .
- D Relative abundance of endogenous ESCO2 and ectopic GFP-ESCO2 in wild-type and ESCO2 knock-out HeLa cells, respectively, as determined by anti-ESCO2 immunoblotting.
- E Relative abundance of ESCO2 in wild-type, bi-allelic and mono-allelic  $\Delta$ A or  $\Delta$ B mutants in HeLa whole-cell extracts. The mutants were generated using CRISPR-Cas9 modification of the endogenous locus. Bi-allelic mutants represent homozygous modification. Mono-allelic mutants represent intended modification at one of the two alleles and a truncation and premature stop codon in the other allele.
- F Representative examples of metaphase chromosome spread from HeLa cells. From left to right: normal (wild-type ESCO2), railroad and loss-of-cohesion phenotypes ( $\Delta$ A/ $\Delta$ A ESCO2). Scale bar, 10  $\mu\text{m}$ .
- G Metaphase chromosome spread analysis from wild-type or ESCO2 mutant HeLa cells modified at the endogenous ESCO2 locus. Error bars represent (–) SD based on two independent blind experiments, each with  $n \geq 100$ .
- H Immunoblot analysis of SMC3(ac) and SMC3 in chromatin fractions from wild-type or endogenously modified mutant ESCO2 HeLa cells treated with control (firefly Gl2 luciferase) or ESCO1 siRNA and synchronized in G2 phase by single thymidine arrest and release for 6 h.

**An ESCO2 mutant defective in MCM binding can mediate centromeric cohesion if tethered to centromeric chromatin**

Our results so far implied that ESCO2-MCM interactions promote cohesion by recruiting ESCO2 to chromatin. To test this hypothesis, further we analysed whether tethering ESCO2 to centromeric chromatin could alleviate the effect of PBM-A deletion on centromeric cohesion. For this purpose, we used ESCO2 deficient in both PBM-A and PBM-B because this mutant had failed to mediate centromeric cohesion even when overexpressed from a cDNA in RBS cells. We N-terminally tagged this mutant with the DNA binding domain of the centromere protein CENPB (Yoda *et al*, 1992), resulting in a CENPB<sup>1–160</sup>-GFP-ESCO2- $\Delta$ AB fusion protein, and stably expressed it in RBS cells.

Immunofluorescence microscopy revealed that this protein was recruited to centromeres, as judged by co-localization with anti-centromeric antibodies (ACA, Fig 7C). Remarkably, this ESCO2 mutant could restore centromeric cohesion almost as well as wild-type ESCO2 (Fig 7B). Mutation of an amino acid residue required for the acetyltransferase activity and cohesion function of ESCO2 (W539G; Gordillo *et al*, 2008; van der Lelij *et al*, 2009) abolished this effect, indicating that it depends on ESCO2's enzymatic activity and is not caused by overexpression of CENPB's DNA binding domain or other artificial properties of this fusion protein. These results support the hypothesis that ESCO2-MCM interactions promote centromeric cohesion by recruiting ESCO2 to chromatin.

Interestingly, when ESCO1 was tethered to centromeres by expressing a CENPB<sup>1–160</sup>-GFP-ESCO1 fusion, centromeric cohesion was only partially restored (Fig 8G–I). Because exchanging the C-terminal acetyltransferase domains of ESCO1 and ESCO2 does not detectably compromise the functions of these enzymes (Alomer *et al*, 2017), it might be an additional feature of ESCO2's N terminus other than PBM-A and PBM-B that contributes to its ability to mediate centromeric cohesion.

**ESCO2-MCM interactions are important for SMC3 acetylation on nascent DNA**

Because cohesion can normally only be established during DNA replication, we investigated whether ESCO2-MCM interactions promote cohesin acetylation at replication forks. First, we addressed

whether ESCO2 is recruited to chromatin via MCM binding before or after replisome activation, which occurs around the same time as ESCO2 synthesis. Note that our MS experiments could not distinguish between these possibilities, as they had revealed that ESCO2 interacts both with MCM (which is part of pre-replicative complexes and replisomes) and with proteins that are part of the replisome, such as CDC45, GINS, RFC and claspin (Figs 2A and EV1C). We therefore analysed whether ESCO2-chromatin interactions depend on DNA replication. For this purpose, we synchronized RBS cells with aphidicolin, inhibited replisome activation with the CDC7 inhibitor PHA767491 and measured the interaction of GFP-ESCO2 with chromatin by FRAP. Under these conditions, GFP-ESCO2 associated with chromatin even longer than in the absence of CDC7 inhibitor (Fig EV4A–D), indicating that replisome activation is not required for ESCO2's recruitment to chromatin, consistent with results in *Xenopus* egg extracts (Higashi *et al*, 2012). Similarly, the association of GFP-ESCO2 with chromatin was unaffected by depletion of CDC45, a member of the CMG helicase, even though this treatment inhibited DNA replication and decreased PCNA levels on chromatin (Fig EV4E–G). These results, together with our MS experiments, indicate that ESCO2 can associate with MCM in both pre-RCs and active replisomes. Furthermore, our FRAP results imply that ESCO2-chromatin interactions become more dynamic during replication fork firing.

Second, to test more directly whether ESCO2 remains associated with MCM after replisome activation, we performed isolation of proteins on nascent DNA (iPOND) experiments in HeLa cells to analyse whether ESCO2 is enriched on newly synthesized DNA, as are replisome components (Sirbu *et al*, 2011). Nascent DNA was labelled with a 10-min 5-ethynyl-2'-deoxyuridine (EdU) pulse and formaldehyde cross-linked to associated proteins, either immediately or after replication had proceeded for 30 min in the absence of EdU ("chase"; Fig 9A). Labelled DNA was then biotinylated and captured, and associated proteins analysed by immunoblotting. As reported in Sirbu *et al*, 2011; PCNA was enriched on nascent DNA but reduced upon "chase", presumably reflecting replisome movement, whereas the core histone H3 increased upon "chase" due to nucleosome formation (Fig 9B and C). Importantly, both endogenous ESCO2 (Fig 9B) and ectopic GFP-ESCO2 (Fig 9C) were also present on nascent DNA and reduced upon "chase", although not to the same extent as PCNA [note that consistent with our results, a

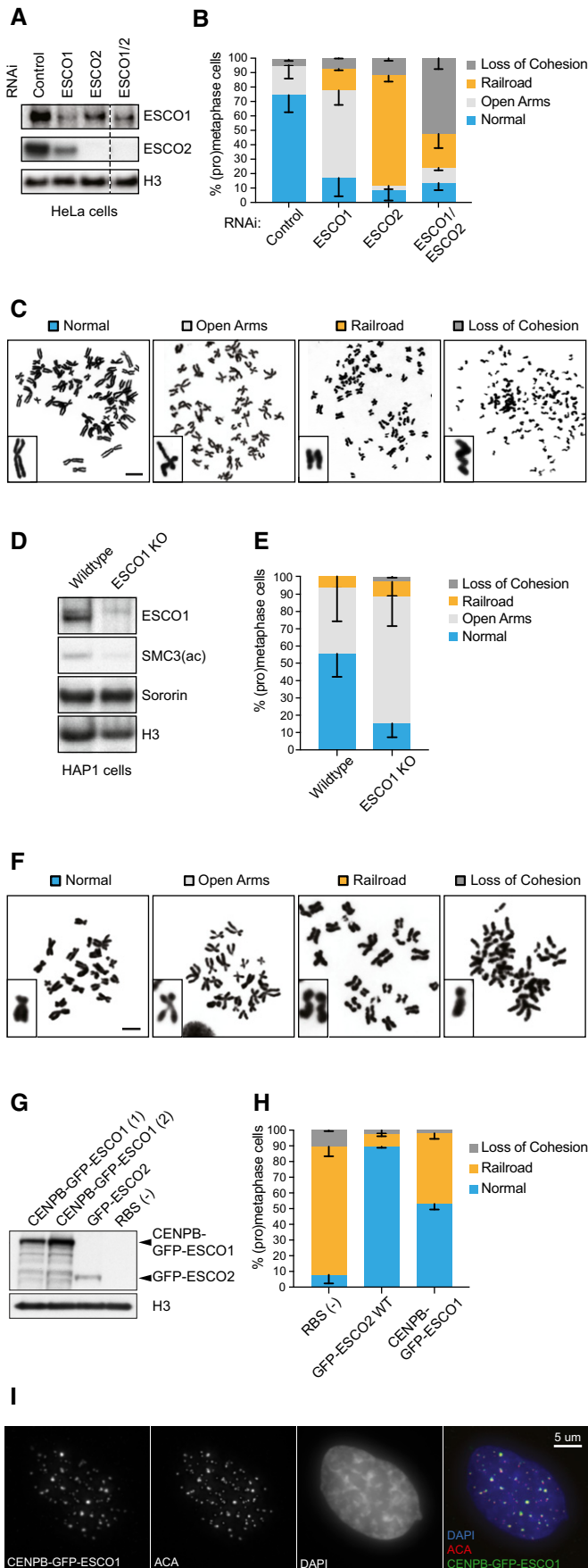


**Figure 8. ESCO1 and ESCO2 have specific functions in arm and centromeric cohesion, respectively.**

- A Immunoblot analysis of chromatin fractions of HeLa cells depleted for ESCO1, ESCO2, or both.
- B Prometaphase/metaphase chromosome spread analysis from ESCO-depleted HeLa cells. Error bars represent (–) SD based on two independent blinded experiments, each with  $n \geq 100$ .
- C Examples of (pro)metaphase chromosome phenotypes. Scale bar, 10  $\mu\text{m}$ .
- D Immunoblot analysis of whole-cell extracts of wild-type and ESCO1 knock-out HAP1 cells.
- E Prometaphase/metaphase chromosome spread analysis from wild-type and ESCO1 knock-out HAP1 cells. Error bars represent (–) SD based on two independent blind experiments, each with  $n \geq 100$ .
- F Examples of (pro)metaphase chromosome phenotypes. Scale bar, 10  $\mu\text{m}$ .
- G Immunoblot analysis of whole-cell extracts of RBS cells expressing ectopic CENPB<sup>1-160</sup>-GFP-ESCO1 (two independent pools) or ESCO2 constructs.
- H Prometaphase/metaphase chromosome spread analysis from RBS cells expressing wild-type GFP-ESCO2 or CENPB<sup>1-160</sup>-GFP-ESCO1 from cDNA. Error bars represent (–) SD based on two independent blind experiments, each with  $n \geq 100$ .
- I CENPB<sup>1-160</sup>-GFP-ESCO1 constitutively expressed from a plasmid in RBS cells localizes to centromeres. CENPB<sup>1-160</sup>-GFP-ESCO1 and centromeres were visualized using GFP and anti-centromeric antibodies (ACA), respectively.

previous study had detected ESCO2 on nascent chromatin in S phase, Alabert *et al*, 2014; however, in this iPOND experiment, the “chase” extended into late S/G2 phase, making it difficult to know whether ESCO2 was reduced under “chase” conditions by replisome movement or ESCO2 degradation which occurs in G2 phase, (van der Lelij *et al*, 2009)]. In the absence of EdU labelling, little or no ESCO2, PCNA and H3 could be detected (last lanes in Fig 9B and C), indicating that these proteins interacted specifically with nascent DNA. Only for MCM, no change could be seen in two independent experiments, possibly due to the high abundance of MCM which could lead to non-specific crosslinking of MCM to DNA even when the replisomes have been chased away. These results are consistent with the hypothesis that ESCO2 translocates with replisomes.

Third, to test this hypothesis further, and to address whether ESCO2’s movement with replisomes is functionally relevant, we analysed whether ESCO2-dependent cohesin acetylation occurs on newly synthesized DNA. For this purpose, we released HeLa cells synchronized at the G1-S transition for 1 h into S phase in the presence of bromodeoxyuridine (BrdU) and analysed the genomic distribution of SMC3(ac) and BrdU by ChIP-seq and DNA immunoprecipitation-sequencing (DIP-seq), respectively (Fig 9D, for SMC3(ac) antibody specificity see Nishiyama *et al*, 2010 and Appendix Figure S4A). For comparison, the distribution of all cohesin complexes was analysed by SMC3 ChIP-seq. As in Fig 7H, we analysed both control HeLa cells and ESCO1-depleted cells in this experiment, to be able to assess ESCO2’s contribution to cohesin acetylation. Furthermore, we compared cells expressing wild-type ESCO2 with those in which ESCO2’s PBM-A motif had been deleted to analyse the importance of ESCO2-MCM interactions for cohesin acetylation during DNA replication (we did not perform the same experiment with cells in G1 phase because ESCO2 is undetectable and cohesin acetylation only depends on ESCO1 in this cell cycle phase; Minamino *et al*, 2015).

As expected, the highest degree of cohesin acetylation could be detected in control cells, i.e. in cells containing both ESCO1 and ESCO2 (Fig 9E). In these, the ratio between the numbers of SMC3 (ac) peaks and the SMC3 peaks was 67%, whereas depletion of ESCO1 and/or deletion of ESCO2’s PBM-A motif reduced this ratio,

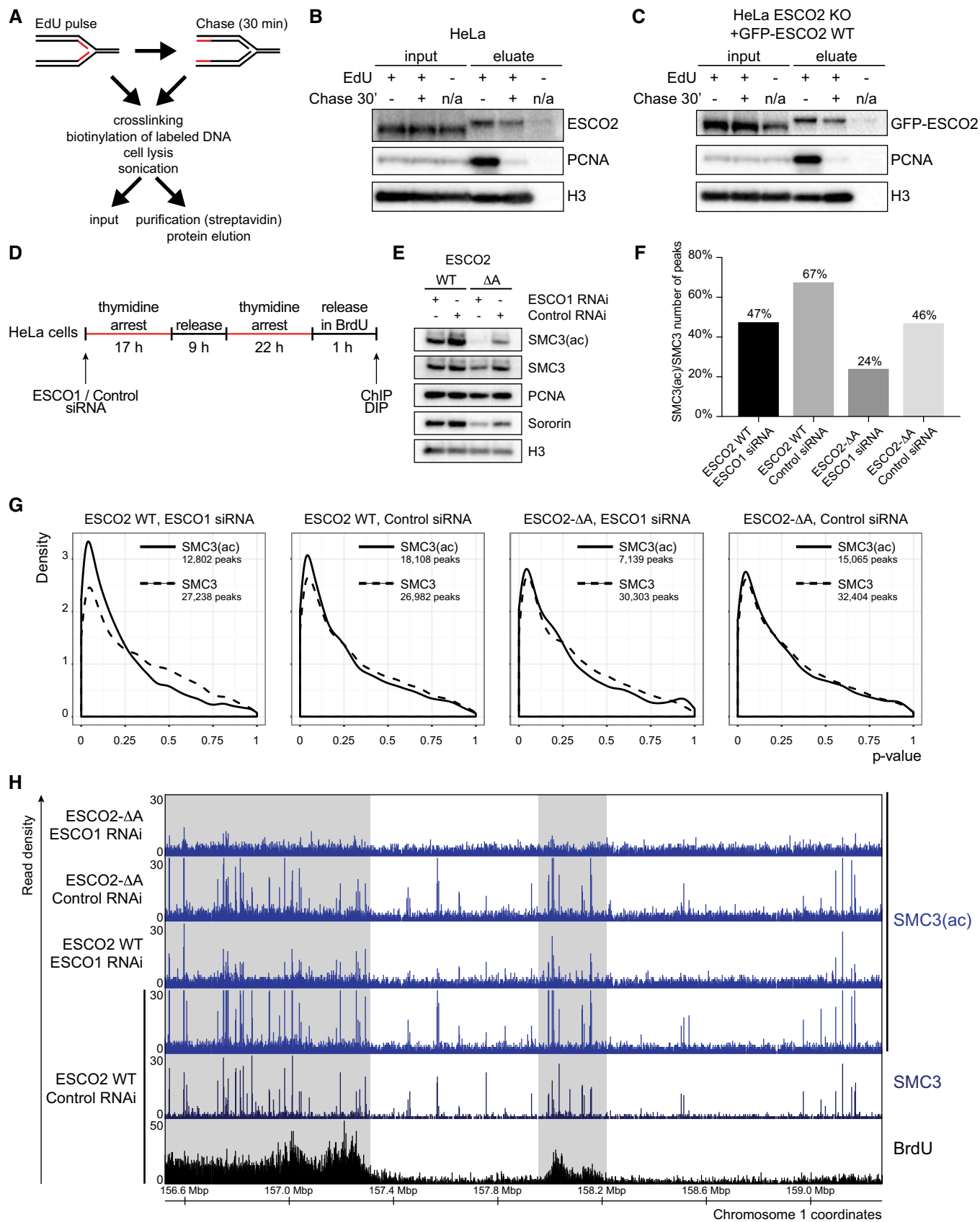


Figure 9.

**Figure 9. ESCO2 might acetylate cohesin at the replication fork in a manner that depends on its interaction with MCM.**

- A iPOND experimental outline.
- B iPOND immunoblot analysis of endogenous ESCO2 in HeLa cells synchronized in mid-S phase. Note that the electrophoretic mobility of ESCO2 in the eluates might be reduced due to a lower lithium dodecyl sulphate concentration in these samples.
- C iPOND immunoblot analysis of ectopic GFP-ESCO2 in HeLa ESCO2 knock-out cells synchronized in mid-S phase.
- D Experimental outline for chromatin immunoprecipitation (ChIP) and DNA immunoprecipitation (DIP) from S phase synchronized HeLa cells treated with ESCO1 or control (luciferase) siRNA.
- E SDS-PAGE-immunoblot analysis of chromatin fractions of HeLa cells expressing ESCO2 wild-type or ESCO2- $\Delta$ A and treated with ESCO1 or control siRNA.
- F Ratios between the numbers of SMC3(ac) and SMC3 peaks in the four experimental conditions.
- G IntervalStats *P*-value distributions of SMC3(ac) peaks (continuous lines) and SMC3 peaks (dashed lines) relative to BrdU peaks in the four outlined experimental conditions. SMC3(ac) correlation with BrdU is highest after ESCO1 depletion, i.e. under conditions in which predominantly ESCO2 is present.
- H Example of ChIP-seq profiles of BrdU, SMC3 and SMC3(ac). Regions with enriched BrdU signal are highlighted with a grey background. For complete set of tracks from the four conditions, see Appendix Fig S4B and S4C.

in cells only expressing ESCO2- $\Delta$ A down to 24% (Fig 9F). These results confirm that both ESCO1 and ESCO2 contribute to cohesin acetylation, that ESCO2's PBM-A motif has an important role in this process, and indicate that the SMC3(ac) antibodies used for ChIP-seq specifically recognized acetylated cohesin and not simply unmodified cohesin with lower affinity.

To determine whether ESCO2-dependent cohesin acetylation occurs on newly replicated DNA, we identified sites enriched in ChIP-seq or DIP-seq reads by the BayesPeak algorithm and determined the co-occurrence of SMC3 or SMC3(ac) signals with BrdU via IntervalStats. Interestingly, this analysis revealed higher correlation between SMC3(ac) and BrdU in cells only expressing wild-type ESCO2, i.e. depleted of ESCO1, than in cells expressing both acetyltransferases (Fig 9G, statistical comparison in Appendix Table S4). Manual inspection of the ChIP-seq and DIP-seq profiles confirmed these results because it showed that ESCO1 depletion from cells expressing wild-type ESCO2 preferentially reduced SMC3(ac) signals in non-replicated regions, whereas SMC3(ac) peaks in replicated regions were only strongly reduced when ESCO1 was depleted from cells expressing ESCO2- $\Delta$ A (Fig 9H, Appendix Fig S4B and S4C, and Appendix Table S4). These observations are consistent with the hypothesis that ESCO2 contributes predominantly to SMC3(ac) at replicated regions.

In line with this, cells expressing ESCO2- $\Delta$ A had numerous SMC3(ac) peaks, but the overall correlation with BrdU regions declined notably (Fig 9G, Appendix Table S4), indicating that the specific cohesin acetylation on newly replicated chromatin depends strongly on ESCO2's PBM-A motif and thus presumably on its ability to interact with the MCM helicase. However, we cannot exclude that ESCO2 also contributes to some cohesin acetylation on non-replicated DNA, as ESCO1 depletion did not abolish all SMC3(ac) peaks in genomic regions that had not or only poorly been replicated (for an example, see right hand side of the locus shown in Fig 9H and Appendix Fig S4B). Alternatively, it is possible that the persistence of these peaks was due to incomplete ESCO1 depletion or partial replication of these regions in a subset of cells. In either case, these results support the hypothesis that ESCO2's ability to bind to MCM contributes directly to replication-coupled cohesin acetylation.

## Discussion

Sister chromatid cohesion is thought to be established by the entrapment of nascent sister chromatids inside cohesin rings. However, this process is not sufficient to hold sister chromatids

together from their synthesis in S phase until their separation in anaphase. Cohesive cohesin complexes also need to be protected from WAPL which can open an "exit gate" between the SMC3 and SCC1 subunits of cohesin and can thereby release cohesin from DNA (Gandhi *et al*, 2006; Kueng *et al*, 2006; Chan *et al*, 2012; Buheitel & Stemmann, 2013; Eichinger *et al*, 2013; Gligoris *et al*, 2014; Huis in 't Veld *et al*, 2014). Preventing this precocious release, which would destroy cohesion again, and not cohesion establishment *per se* (Skibbens *et al*, 1999; Tóth *et al*, 1999; Rowland *et al*, 2009), appears to be the key function of SMC3 acetylation (Nishiyama *et al*, 2010; Chan *et al*, 2012; Lopez-Serra *et al*, 2012; Ladurner *et al*, 2016). Previous analyses of Eco1 in budding yeast (Lengronne *et al*, 2006; Moldovan *et al*, 2006; Borges *et al*, 2013) and the functional characterization of human ESCO2-replisome interactions reported here suggest that also this protection from WAPL by SMC3 acetylation occurs in the direct vicinity of replication forks. Cohesion establishment and SMC3 acetylation by ESCO2 might be tightly coupled in space and time to protect cohesin complexes from WAPL immediately after they have established cohesion.

In addition, it is possible that the recruitment of ESCO2 to replication forks helps to ensure that only cohesive cohesin complexes become acetylated by this enzyme. The latter scenario could be important to enable the stabilization of cohesive cohesin on chromatin without broadly modifying non-cohesive cohesin complexes that are thought to be important determinants of higher-order chromatin structure and gene regulation by forming chromatin loops *in cis* (Hadjur *et al*, 2009; Nativio *et al*, 2009; Kagey *et al*, 2010; Schwarzer *et al*, 2017; Gassler *et al*, 2017; Rao *et al*, 2017; Wutz *et al*, 2017). It is conceivable that interactions between these latter complexes and DNA need to be maintained in a dynamic, WAPL-regulatable state to enable dynamic changes in chromatin structure (Tedeschi *et al*, 2013). Directly coupling cohesin acetyltransferases to replisomes could be a mechanism that creates such specificity for cohesive cohesin.

Previous work had shown that human ESCO2 can bind to PCNA (Moldovan *et al*, 2006), but our unbiased proteomic analysis of 55 cohesion and DNA replication proteins did not identify ESCO2-PCNA interactions in human cells, and live-cell confocal imaging of GFP-ESCO2 and RFP-PCNA did not reveal overlap in their localization (Appendix Fig S3A). We did, however, confirm the previous observation (Higashi *et al*, 2012) that mutation of ESCO2's putative PCNA interaction sequence (PIP box) partially compromises ESCO2's cohesion function (Fig 7B). Interactions between ESCO2 and PCNA must therefore either be transient, which could explain

why they were undetectable in our experiments, or ESCO2's PIP box has a function independent of PCNA. Consistent with the latter possibility, it has been pointed out that PIP motifs can interact with proteins other than PCNA (Boehm & Washington, 2016).

Instead, our results show that on chromatin in replicating cells ESCO2 associates, presumably in stoichiometric amounts, with MCM, the motor of the CMG replicative helicase. This interaction can explain the previous observation that pre-RCs are required for recruitment of ESCO2 to chromatin in *Xenopus* egg extracts (Higashi et al, 2012). Importantly, our MS analyses also identified interactions between ESCO2 and components of active replisomes, suggesting that ESCO2 might travel with replisomes during DNA replication to mediate acetylation of cohesin. The observation that ESCO2 associates with nascent chromatin (Alabert et al, 2014; Fig 9A–C) and acetylates cohesin on newly replicated DNA (Fig 9D–H) provides support for this hypothesis.

It is interesting to note that most of ESCO2's N-terminal domain is predicted to be unstructured, in which case it could extend over more than 100 nm. This could be long enough to allow the acetylation of cohesin complexes that have entrapped sister DNAs, which are synthesized behind replication forks, whereas MCM is thought to travel at its front. At the same time, ESCO2's N-terminal domain could function as a “leash” that restricts the range in which its catalytic domain can acetylate cohesin. This could create specificity for cohesin complexes, very much like a flexible linker in the chromosome passenger complex has been proposed to limit the range in which Aurora B can phosphorylate substrate proteins at kinetochores (Liu et al, 2009; reviewed in Krenn & Musacchio, 2015). Alternatively, it is possible that ESCO2 would acetylate cohesin complexes that are about to establish cohesion in front of the replication fork, to pre-empt the possibility that they would be released by WAPL again.

Somewhat surprisingly, we observed that tethering ESCO2 to centromeres is sufficient to restore centromeric cohesion in RBS cells that lack ESCO2. This finding does not exclude the possibility that ESCO2 normally travels with active replisomes, but implies that this association with translocating replisomes is not essential for centromeric cohesion under all conditions. We suspect that this result is related to another unexpected observation that we made namely that ESCO2 mutants deficient in MCM binding could restore centromeric cohesion if they were overexpressed, whereas the function of these mutants was compromised when they were expressed at normal levels from endogenous alleles modified by CRISPR-Cas9 genome editing. These results imply that ESCO2 levels are critically important, a notion that is supported by the finding that both Eco1 and ESCO2 levels are controlled at the transcriptional and protein stability levels (van der Lelij et al, 2009; Lafont et al, 2010; Lyons & Morgan, 2011; Whelan et al, 2012b; Lyons et al, 2013). We suspect that ESCO2 levels are limited to a concentration that requires MCM binding for efficient cohesin acetylation, in order to ensure that only cohesin becomes acetylated. On the technical side, our results emphasize the great importance of analysing proteins at their physiological concentrations.

In contrast to ESCO2 purifications, ESCO1 samples isolated from chromatin in S phase cells contained only a few peptides of MCM subunits, whereas no ESCO1 was detected in MCM purifications. Although this result raises the possibility that ESCO1 may also transiently associate with MCM, we consider it more plausible to think

that ESCO1 is recruited to chromatin differently than ESCO2. This notion is consistent with the absence of the MCM interaction motif PBM-A in ESCO1 (Higashi et al, 2012), reported interactions between ESCO1 and PDS5 proteins (Minamino et al, 2015), the presence of ESCO1 at genomic cohesin binding sites (Rahman et al, 2015) and ESCO1's ability to acetylate cohesin independent of DNA replication (Minamino et al, 2015). Our observation that cohesin acetylation in non-replicated regions depends largely on ESCO1 (Fig 9H) further supports this notion.

Despite these differences, ESCO1 must be able to protect sufficient amounts of cohesin from WAPL to enable cell proliferation, as ESCO2-deficient RBS cells are viable and in rare cases even patients are alive. Conversely, our results obtained with haploid cells lacking ESCO1 show that also ESCO1 is dispensable for cell viability, implying that also ESCO2 alone is sufficient for cellular survival, consistent with the observation that in *Xenopus* egg extracts cohesin acetylation and cohesion maintenance occur in the absence of ESCO1 (Higashi et al, 2012). These findings underscore the partial redundancy of ESCO1 and ESCO2, recently also observed in chicken cells (Kawasumi et al, 2017), yet both enzymes clearly also have specific functions. This was well known for ESCO2's role in centromere cohesion, but has now been expanded by our observation that ESCO1 is particularly important for proper levels of arm cohesion. What determines this partial spatial diversification in function, and whether ESCO1-mediated cohesin acetylation before DNA replication serves functions other than cohesion maintenance will be important questions for future studies.

## Materials and Methods

### Cell culture, transfections and cell synchronization

HeLa Kyoto or immortalized fibroblasts from Roberts syndrome patient (VU1199-F SV40) (van der Lelij et al, 2009) were cultured in DMEM supplemented with 10% FBS (Gibco/Thermo Fisher Scientific, 10500-064), 0.2 mM L-glutamine (Sigma-Aldrich, G7513), 100 U/ml penicillin and 100 µg/ml streptomycin (Sigma-Aldrich, P0781). Transformants were selected with 500 µg/ml geneticin (Gibco, 11811) or 1 µg/ml puromycin (Sigma-Aldrich, P9620). RBS cells were transfected with FuGene (Promega, E2311) and plasmid DNA. HeLa Kyoto cells were transfected with Lipofectamine 2000 (Thermo Fisher, 11668019), and plasmid DNA. siRNA was transfected with RNAiMAX (Thermo Fischer, 13778). RBS cells were synchronized by arrest in S phase with 1.2 µg/ml aphidicolin (Sigma-Aldrich, A0781) for 20–24 h. HeLa Kyoto cells were synchronized by arrest in S phase with 2 mM thymidine (Sigma-Aldrich, T1895) for 20–24 h unless noted otherwise. Media were supplemented with 20 µM PHA-767491 to inhibit CDC7 kinase for 4 h.

### LAP immunoprecipitation

Cells synchronized in S phase by a thymidine treatment were released for 2.5 h to mid-S phase and harvested. Pellets were resuspended in lysis buffer and used for single-step anti-GFP-IP directly or after separation of soluble and chromatin-bound fractions. The



beads coupled to anti-GFP antibody and bound to LAP-tagged proteins were extensively washed, and captured proteins were eluted with 0.1 M glycine, and eluates were neutralized with 1.5 M Tris-HCl pH9.2. See Appendix for details. See Appendix also for details about LAP/GFP-IP cross-linking.

### Mass spectrometry

Immunoprecipitated samples were reduced, alkylated and trypsin-digested in solution or on beads (when cross-linked, CL). CL peptides were enrichment with size-exclusion chromatography. Samples for identification, quantification or CL mass spectrometry were analysed by Orbitrap XL, VelosPro or QExactive mass spectrometers. See Appendix for technical details and data analysis.

### Mutagenesis

ESCO2 mutants were generated from GFP-ESCO2 cloned in pIRESneo3 (van der Lelij *et al*, 2009). Motif A was deleted by PCR splicing. Deletion of motif B and mutation of PIP box were obtained by quick change PCR. CENPB residues 1–160 were cloned upstream from GFP-ESCO2 mutants or GFP-ESCO1.

### CRISPR/Cas9-mediated genome engineering

HeLa Kyoto cells expressing motif A-deleted or motif B-deleted versions of ESCO2 were generated by CRISPR-mediated homologous recombination as described (Cong *et al*, 2013). Cells were transfected with two plasmids expressing nickase SpCas9(D10A)-2A-EGFP and chimeric guide RNAs (motif A gRNA combination 1: GTGGAGAGCGCAGATTTAAA and GAAGTGGTACCTCAATCCAC; motif A gRNA combination 2: GTGGTTGTAAAAAGATACAG and GAAGTGGTACCTCAATCCAC; motif B: GAAAAAATGCTGCTCACCC and GTCTCTTAGAAAATCGTCCC), as well as a homology plasmid that carried the deletions flanked on either side by 330–950 nucleotides surrounding the deletion sites that were generated from HeLa genomic DNA by PCR (forward primer: CTACCCAGGA AAAGCCCCAG; reverse primer: TGGCTTTATAAAAGCAGTCCAGA). Clonal cell lines were generated by FACS and recombination and homozygous tagging was assayed by PCR (forward primer TGGCAGCTCTTACTCCAAGG; reverse primer: ACTAAACACTATGCTATCTGGCT) followed by blunt-end cloning (CloneJET PCR Cloning Kit, Thermo Fisher, Cat# K1231) and Sanger sequencing of single colonies. As a result, we obtained one homozygous ESCO2- $\Delta A$  clone ( $\Delta A/\Delta A$ ; bi-allelic expression), one hemizygous ESCO2- $\Delta A$  clone with one allele leading to premature STOP codon, a tetraploid clone ( $\Delta A/-$ ; mono-allelic expression), one homozygous ESCO2- $\Delta B$  clone ( $\Delta B/\Delta B$ ; bi-allelic expression), one hemizygous ESCO2- $\Delta B$  clone ( $\Delta B/-$ ; mono-allelic expression) and one ESCO2 knock-out clone ( $\Delta/\Delta$ ).

### Fluorescence recovery after photobleaching

Cells for FRAP experiments were grown on 8-well Lab-Tek II chambered coverglass (Nunc, 734-2061). Fifteen minutes prior to imaging, medium was changed to CO<sub>2</sub>-independent medium without phenol red supplemented with 10% FCS, 0.2 mM L-glutamine, antibiotics and 50  $\mu$ M  $\beta$ -mercaptoethanol (Thermo Fisher Scientific), 1 mg/l cycloheximide and 0.5 mg/l Hoechst 33342. FRAP was

performed on an LSM5 Duo (Zeiss) confocal microscope using a 63 $\times$  Plan-Apochromat objective and open pinhole. Twenty images were acquired before bleaching three times at 100% laser intensity (100 mW diode 488), followed by 500 post-bleach acquisition frames. For circular FRAP, a radial spot ( $r = 2 \mu$ m) was bleached in the nucleus and frames were acquired at 400-ms intervals. For fast-acquisition FRAP, a nuclear area of 15.87  $\mu$ m width and 1.98  $\mu$ m length was imaged, bleaching was performed at half width, and frames were acquired at 9.2-ms intervals. For FRAP in Fig EV4, cells were imaged in FluoroBrite DMEM medium with 10% FBS, 1 $\times$  Glutamax, 1 mM sodium pyruvate, penicillin/streptomycin (Life Technologies) and 50  $\mu$ M  $\beta$ -mercaptoethanol (Millipore) on a Nikon eclipse Ti microscope with Apo TIRF 100 $\times$  objective, Andor iXon  $\times 3$  camera and equipped with a mosaic for spot bleaching using a 405 nm laser, purchased using funds from an NIH S10 Shared Instrumentation Grant (S10RR026775-01) at the Stanford Biochemistry Department. Signal intensities were measured using ImageJ at bleached, nuclear and background regions (circular FRAP) or bleached and unbleached areas (fast-acquisition FRAP) and normalized as described (Ellenberg *et al*, 1997). Data were analysed using Berkeley Madonna and a sum of two exponential functions that represent nuclear diffusing ( $k_{Diff}$ ) and chromatin-bound populations ( $B$ ;  $k_{Bind}$ );  $f(t) = (1-B)*(1-EXP(-k_{Diff}*t)) + B*(1-EXP(-k_{Bind}*t))$ .

### Chromatin immunoprecipitation

MCM3, ESCO2 (mutants) and SMC3 ChIPs, and BrdU-DIP were performed as in Ladurner *et al* (2016). SMC3(ac) was performed as in Schmidt *et al* (2009). See Appendix for technical details and data analysis.

### Chromosome spreads

Logarithmically growing cells were treated with 300 nM nocodazole (Sigma, M1404) for 40 min (or 15 min in Fig 8B and C and 30 min in Fig 8E and F) before mitotic shake-off in PBS, hypotonic treatment with 1.75 volumes of tap water, fixation and washing with 75% methanol/25% acetic acid, spreading on glass slides and staining with 4% Giemsa. Phenotypes were scored blind in two biological replicates with at least 100 metaphase plates counted per mutant per replicate. Chromosome spread phenotypes were counted when more than half of the chromosomes from one cell showed a particular phenotype, except for the spreads shown in Fig 8, where at least three chromosomes from one cell had to show “open arms” or “railroad” phenotypes.

Isolation of proteins on nascent DNA (iPOND) was performed according to Sirbu *et al* (2012). See Appendix for details.

Immunofluorescence microscopy, confocal microscopy, time-lapse spinning-disc microscopy, and flow cytometry, see Appendix for details.

The following antibodies were used for immunoblot analysis:

- Anti- $\alpha$ -tubulin, mouse (Sigma-Aldrich, T5168)
- Anti-histone H3, rabbit (Cell Signaling, 9715L)
- Anti-GFP, goat (Poser *et al*, 2008)
- Anti-GFP, mouse (Roche, 11814460001)
- Anti-ESCO2, guinea pig (van der Lelij *et al*, 2009)

Anti-acetyl-SMC3, mouse (gift from K. Shirahige (Nishiyama *et al*, 2010)  
 Anti-SMC3, rabbit (Bethyl Laboratories, A300-060A)  
 Anti-SMC1, rabbit (Bethyl Laboratories, A300-055A)  
 Anti-MCM2, mouse (Becton Dickinson, 610700)  
 Anti-PCNA, mouse (Santa Cruz, sc-56)  
 Anti-CDC45, rabbit (Cell Signaling, 3673)  
 Anti- $\gamma$ -tubulin, mouse (Sigma, T5326)  
 Anti-H3, rabbit (Abcam, ab1791)  
 Anti-Sororin, rabbit (A953, SPTKPLRRSQRKSGSELPSC-C)  
 Anti-ESCO1, mouse (Minamino *et al*, 2015; Fig 8A)  
 Anti-ESCO1, rabbit (A782, KSKENSSKVTKKSDDKNSE-C, Fig 8D)

The following siRNAs were used (40 nM):

ESCO1: sense 5'-GAGAAUAAUUUCCAGGUUtt-3'  
 ESCO2: sense 5'-GAAAGAACGUGUAGUAGCAtt-3'  
 Gl2 (Luciferase): sense 5'-CGUACGCGGAUACUUCGAtt-3'  
 CDC45 smart pool On-TARGETplus, Dharmacon, L-003232-00.  
 Non-targeting pool On-TARGETplus, Dharmacon, D-001810-10.

**Expanded View** for this article is available online.

## Acknowledgements

We wish to thank Susanne Opravil and Ines Steinmacher for MS sample preparation; Elisabeth Roitinger for cohesin acetylation MS; Kristina Uzunova, Pim Huis in 't Veld, Robert Mahen, Gerhard Dürnberger, Kota Nagasaka, and the laboratories of Johan de Winter, Johannes Zuber, Daniel Gerlich, Simon Boulton, and Aaron Straight for providing materials and expertise. We further thank the IMP/IMBA protein chemistry facility for MS, VBCF NGS Unit ([www.vbcf.ac.at](http://www.vbcf.ac.at)) for deep sequencing, and the IMP/IMBA Biooptics facility and members of the J.-M.P. group for discussions and assistance. Research in the laboratory of J.-M.P. is supported by Boehringer Ingelheim, the Austrian Science Fund (FWF special research program SFB F34 "Chromosome Dynamics" and Wittgenstein award Z196-B20), the Austrian Research Promotion Agency (Headquarter grants FFG-834223 and FFG-852936, Laura Bassi Centre for Optimized Structural Studies grant FFG-840283), the Vienna Science and Technology Fund (WWTF LS09-13), the European Community's Seventh Framework Programme (FP7/2007-2013) under grant agreement 241548 (MitoSys) and the European Research Council (ERC) under the European Union's Horizon 2020 research and innovation programme GA No 693949. The initial phase of this project was funded by the European Community's Sixth Framework Programme (FP6) under grant agreement 503464 (MitoCheck).

## Author contributions

J-MP conceived the project. MPI performed protein purifications for proteomic screening, CLMS and qMS; generated and characterized ESCO2 mutants and CRISPR-Cas9 modified cell lines; and performed CMG inhibition, iPOND, ChIP-seq and DIP-seq experiments. RL performed FRAP experiments and analysed FRAP data. RB and ER performed CLMS and CLMS data analysis. IP and AAH generated LAP-tagged cell pools, OH analysed proteomic screen, quantitative and cross-linking MS data, MN generated Circos plots, 3D-models and ESCO2 structure predictions, GW performed ESCO1/ESCO2 depletion-chromosome spread experiments, PvdL performed the HAP1 experiments, J-KH and JE performed proteomic screen interactome analysis, EK made the initial observation of the ESCO2-MCM interaction, JRAH designed the replisome screen cell pool set, HA-E analysed ChIP/DIP data. KM supervised all MS experiments and their data analyses. MPI and J-MP designed the experiments, interpreted data and wrote the manuscript.

## Conflict of interest

The authors declare that they have no conflict of interest.

## References

- Alabert C, Bukowski-Wills J-C, Lee S-B, Kustatscher G, Nakamura K, de Lima Alves F, Menard P, Mejlvang J, Rappsilber J, Groth A (2014) Nascent chromatin capture proteomics determines chromatin dynamics during DNA replication and identifies unknown fork components. *Nat Cell Biol* 16: 281–293
- Alomer RM, da Silva EML, Chen J, Piekarz KM, McDonald K, Sansam CG, Sansam CL, Rankin S (2017) Esco1 and Esco2 regulate distinct cohesin functions during cell cycle progression. *Proc Natl Acad Sci USA* 114: 9906–9911
- Ansbach AB, Noguchi C, Klansek IW, Heidlebaugh M, Nakamura TM, Noguchi E (2008) RFCctf18 and the Swi1-Swi3 complex function in separate and redundant pathways required for the stabilization of replication forks to facilitate sister chromatid cohesion in *Schizosaccharomyces pombe*. *Mol Biol Cell* 19: 595–607
- Beckouët F, Srinivasan M, Roig MB, Chan K-L, Scheinost JC, Batty P, Hu B, Petela N, Gligoris T, Smith AC, Strmecki L, Rowland BD, Nasmyth K (2016) Releasing activity disengages cohesin's Smc3/Sccl interface in a process blocked by acetylation. *Mol Cell* 61: 563–574
- Ben-Shahar TR, Heeger S, Lehane C, East P, Flynn H, Skehel M, Uhlmann F (2008) Eco1-dependent cohesin acetylation during establishment of sister chromatid cohesion. *Science* 321: 563–566
- Boehm EM, Washington MT (2016) R.I.P. to the PIP: PCNA-binding motif no longer considered specific: PIP motifs and other related sequences are not distinct entities and can bind multiple proteins involved in genome maintenance. *BioEssays* 38: 1117–1122
- Borges V, Smith DJ, Whitehouse I, Uhlmann F (2013) An Eco1-independent sister chromatid cohesion establishment pathway in *S. cerevisiae*. *Chromosoma* 122: 121–134
- Brand N, Faul T, Grummt F (2007) Interactions and subcellular distribution of DNA replication initiation proteins in eukaryotic cells. *Mol Genet Genomics* 278: 623–632
- Buheitel J, Stemmann O (2013) Prophase pathway-dependent removal of cohesin from human chromosomes requires opening of the Smc3-Sccl gate. *EMBO J* 32: 666–676
- Bürkstümmer T, Banning C, Hainzl P, Schobesberger R, Kerzendorfer C, Pauler FM, Chen D, Them N, Schischlik F, Rebsamen M, Smida M, Fece de la Cruz F, Lapao A, Liszt M, Eizinger B, Guenzl PM, Blomen VA, Konopka T, Gapp B, Parapatics K *et al* (2013) A reversible gene trap collection empowers haploid genetics in human cells. *Nat Methods* 10: 965–971
- Chan K-L, Roig MB, Hu B, Beckouët F, Metson J, Nasmyth K (2012) Cohesin's DNA exit gate is distinct from its entrance gate and is regulated by acetylation. *Cell* 150: 961–974
- Cheeseman IM, Desai A (2005) A combined approach for the localization and tandem affinity purification of protein complexes from metazoans. *Sci STKE* 2005: pl1
- Chikina MD, Troyanskaya OG (2012) An effective statistical evaluation of ChIPseq dataset similarity. *Bioinformatics* 28: 607–613
- Cong L, Ran FA, Cox D, Lin S, Barretto R, Habib N, Hsu PD, Wu X, Jiang W, Marraffini LA, Zhang F (2013) Multiplex genome engineering using CRISPR/Cas systems. *Science* 339: 819–823
- Das M, Singh S, Pradhan S, Narayan G (2014) MCM paradox: abundance of eukaryotic replicative helicases and genomic integrity. *Mol Biol Int* 2014: 574850

- De K, Sterle L, Krueger L, Yang X, Makaroff CA (2014) *Arabidopsis thaliana* WAPL is essential for the prophase removal of cohesin during meiosis. *PLoS Genet* 10: e1004497
- Deegan TD, Diffley JFX (2016) MCM: one ring to rule them all. *Curr Opin Struct Biol* 37: 145–151
- Dewar H, Tanaka K, Nasmyth K, Tanaka TU (2004) Tension between two kinetochores suffices for their bi-orientation on the mitotic spindle. *Nature* 428: 93–97
- Dimitrova DS, Todorov IT, Melendy T, Gilbert DM (1999) Mcm2, but not RPA, is a component of the mammalian early G1-phase prereplication complex. *J Cell Biol* 146: 709–722
- Drozdzetskiy A, Cole C, Procter J, Barton CJ (2015) JPred4: a protein secondary structure prediction server. *Nucleic Acids Res* 43: W389–W394
- Eichinger CS, Kurze A, Oliveira RA, Nasmyth K (2013) Disengaging the Smc3/kleisin interface releases cohesin from *Drosophila* chromosomes during interphase and mitosis. *EMBO J* 32: 656–665
- Ellenberg J, Siggia ED, Moreira JE, Smith CL, Presley JF, Worman HJ, Lippincott-Schwartz J (1997) Nuclear membrane dynamics and reassembly in living cells: targeting of an inner nuclear membrane protein in interphase and mitosis. *J Cell Biol* 138: 1193–1206
- Erico A, Cosentino C, Rivera T, Losada A, Schwob E, Hunt T, Costanzo V (2009) Tipin/Tim1/And1 protein complex promotes Pol alpha chromatin binding and sister chromatid cohesion. *EMBO J* 28: 3681–3692
- Feytout A, Vaur S, Genier S, Vazquez S, Javerzat J-P (2011) Psm3 acetylation on conserved lysine residues is dispensable for viability in fission yeast but contributes to Eso1-mediated sister chromatid cohesion by antagonizing Wpl1. *Mol Cell Biol* 31: 1771–1786
- Fragkos M, Ganier O, Coulombe P, Méchali M (2015) DNA replication origin activation in space and time. *Nat Rev Mol Cell Biol* 16: 360–374
- Frigola J, Remus D, Mehanna A, Diffley JFX (2013) ATPase-dependent quality control of DNA replication origin licensing. *Nature* 495: 339–343
- Gandhi R, Gillespie PJ, Hirano T (2006) Human Wapl is a cohesin-binding protein that promotes sister-chromatid resolution in mitotic prophase. *Curr Biol* 16: 2406–2417
- Gassler J, Brandao HB, Imakaev M, Flyamer IM, Ladstatter S, Bickmore WA, Peters J-M, Mirny LA, Tachibana-Konwalski K (2017) A mechanism of cohesin-dependent loop extrusion organizes zygotic genome architecture. *EMBO J* 2017: 363600–363618
- Gerlich D, Koch B, Dupeux F, Peters J-M, Ellenberg J (2006) Live-cell imaging reveals a stable cohesin-chromatin interaction after but not before DNA replication. *Curr Biol* 16: 1571–1578
- German J (1979) Roberts' syndrome. I. Cytological evidence for a disturbance in chromatid pairing. *Clin Genet* 16: 441–447
- Gligoris TG, Scheinost JC, Bürmann F, Petela N, Chan K-L, Uluocak P, Beckouët F, Gruber S, Nasmyth K, Löwe J (2014) Closing the cohesin ring: structure and function of its Smc3-kleisin interface. *Science* 346: 963–967
- Gordillo M, Vega H, Trainer AH, Hou F, Sakai N, Luque R, Kayserili H, Basaran S, Skovby F, Hennekam RCM, Uzielli MLG, Schnur RE, Manouvrier S, Chang S, Blair E, Hurst JA, Forzano F, Meins M, Simola KOJ, Raas-Rothschild A et al (2008) The molecular mechanism underlying Roberts syndrome involves loss of ESCO2 acetyltransferase activity. *Hum Mol Genet* 17: 2172–2180
- Guacci V, Koshland D, Strunnikov A (1997) A direct link between sister chromatid cohesion and chromosome condensation revealed through the analysis of MCD1 in *S. cerevisiae*. *Cell* 91: 47–57
- Guacci V, Stricklin J, Bloom MS, Guo X, Bhatner M, Koshland D (2015) A novel mechanism for the establishment of sister chromatid cohesion by the ECO1 acetyltransferase. *Mol Biol Cell* 26: 117–133
- Guillou E, Ibarra A, Coulon V, Casado-Vela J, Rico D, Casal I, Schwob E, Losada A, Méndez J (2010) Cohesin organizes chromatin loops at DNA replication factories. *Genes Dev* 24: 2812–2822
- Hadjur S, Williams LM, Ryan NK, Cobb BS, Sexton T, Fraser P, Fisher AG, Merkschlager M (2009) Cohesins form chromosomal cis-interactions at the developmentally regulated IFNG locus. *Nature* 460: 410–413
- Haering CH, Farcas A-M, Arumugam P, Metson J, Nasmyth K (2008) The cohesin ring concatenates sister DNA molecules. *Nature* 454: 297–301
- Hanna JS, Kroll ES, Lundblad V, Spencer FA (2001) *Saccharomyces cerevisiae* CTF18 and CTF4 are required for sister chromatid cohesion. *Mol Cell Biol* 21: 3144–3158
- Heidinger-Pauli JM, Unal E, Koshland D (2009) Distinct targets of the Eco1 acetyltransferase modulate cohesion in S phase and in response to DNA damage. *Mol Cell* 34: 311–321
- Higashi TL, Ikeda M, Tanaka H, Nakagawa T, Bando M, Shirahige K, Kubota Y, Takisawa H, Masukata H, Takahashi TS (2012) The prereplication complex recruits XEco2 to chromatin to promote cohesin acetylation in *Xenopus* egg extracts. *Curr Biol* 22: 977–988
- Hou F, Zou H (2005) Two human orthologues of Eco1/Ctf7 acetyltransferases are both required for proper sister-chromatid cohesion. *Mol Biol Cell* 16: 3908–3918
- Huis in 't Veld PJ, Herzog F, Ladurner R, Davidson IF, Piric S, Kreidl E, Bhaskara V, Aebersold R, Peters J-M (2014) Characterization of a DNA exit gate in the human cohesin ring. *Science* 346: 968–972
- Hutchins JRA, Toyoda Y, Hegemann B, Poser I, Hériché J-K, Sykora MM, Augsburg M, Hudecz O, Buschhorn BA, Bulkescher J, Conrad C, Comartin D, Schleiffer A, Sarov M, Pozniakovskiy A, Slabicki MM, Schloissnig S, Steinmacher I, Leuschner M, Szykora A et al (2010) Systematic analysis of human protein complexes identifies chromosome segregation proteins. *Science* 328: 593–599
- Ishida T, Kinoshita K (2007) PrDOS: prediction of disordered protein regions from amino acid sequence. *Nucleic Acids Res* 35: W460–W464
- Ivanov D, Schleiffer A, Eisenhaber F, Mechtler K, Haering CH, Nasmyth K (2002) Eco1 is a novel acetyltransferase that can acetylate proteins involved in cohesion. *Curr Biol* 12: 323–328
- Jones DT (1999) Protein secondary structure prediction based on position-specific scoring matrices. *J Mol Biol* 292: 195–202
- Kagey MH, Newman JJ, Bilodeau S, Zhan Y, Orlando DA, van Berkum NL, Ebmeier CC, Goossens J, Rahl PB, Levine SS, Taatjes DJ, Dekker J, Young RA (2010) Mediator and cohesin connect gene expression and chromatin architecture. *Nature* 467: 430–435
- Kaufman DG, Cordeiro-Stone M, Brylawski BP, Cohen SM, Chastain PD (2007) Early S phase DNA replication: a search for targets of carcinogenesis. *Adv Enzyme Regul* 47: 127–138
- Kawasumi R, Abe T, Arakawa H, Garre M, Hirota K, Branzei D (2017) ESCO1/2's roles in chromosome structure and interphase chromatin organization. *Genes Dev* 31: 2136–2150
- Kenna MA, Skibbens RV (2003) Mechanical link between cohesion establishment and DNA replication: Ctf7p/Eco1p, a cohesion establishment factor, associates with three different replication factor C complexes. *Mol Cell Biol* 23: 2999–3007
- Krenn V, Musacchio A (2015) The aurora B Kinase in chromosome Bi-orientation and spindle checkpoint signaling. *Front Oncol* 5: 225
- Krzywinski M, Schein J, Birol I, Connors J, Gascoyne R, Horsman D, Jones SJ, Marra MA (2009) Circos: an information aesthetic for comparative genomics. *Genome Res* 19: 1639–1645

- Kueng S, Hegemann B, Peters BH, Lipp JJ, Schleiffer A, Mechtler K, Peters J-M (2006) Wapl controls the dynamic association of cohesin with chromatin. *Cell* 127: 955–967
- Kuipers MA, Stasevich TJ, Sasaki T, Wilson KA, Hazelwood KL, McNally JG, Davidson MW, Gilbert DM (2011) Highly stable loading of Mcm proteins onto chromatin in living cells requires replication to unload. *J Cell Biol* 192: 29–41
- Ladurner R, Kreidl E, Ivanov MP, Ekker H, Idarraga-Amado MH, Busslinger GA, Wutz G, Cisneros DA, Peters J-M (2016) Sororin actively maintains sister chromatid cohesion. *EMBO J* 35: 635–653
- Lafont AL, Song J, Rankin S (2010) Sororin cooperates with the acetyltransferase Eco2 to ensure DNA replication-dependent sister chromatid cohesion. *Proc Natl Acad Sci USA* 107: 20364–20369
- van der Lelij P, Godthelp BC, van Zon W, van Gosliga D, Oostra AB, Steltenpool J, de Groot J, Scheper RJ, Wolthuis RM, Waisfisz Q, Darroudi F, Joenje H, de Winter JP (2009) The cellular phenotype of Roberts syndrome fibroblasts as revealed by ectopic expression of ESCO2. *PLoS One* 4: e6936
- Leman AR, Noguchi C, Lee CY, Noguchi E (2010) Human Timeless and Tipin stabilize replication forks and facilitate sister-chromatid cohesion. *J Cell Sci* 123: 660–670
- Leman AR, Noguchi E (2013) The replication fork: understanding the eukaryotic replication machinery and the challenges to genome duplication. *Genes (Basel)* 4: 1–32
- Lengronne A, McIntyre J, Katou Y, Kanoh Y, Hopfner K-P, Shirahige K, Uhlmann F (2006) Establishment of sister chromatid cohesion at the *S. cerevisiae* replication fork. *Mol Cell* 23: 787–799
- Li N, Zhai Y, Zhang Y, Li W, Yang M, Lei J, Tye B-K, Gao N (2015) Structure of the eukaryotic MCM complex at 3.8 Å. *Nature* 524: 186–191
- Liu D, Vader G, Vromans MJM, Lampson MA, Lens SMA (2009) Sensing chromosome bi-orientation by spatial separation of aurora B kinase from kinetochore substrates. *Science* 323: 1350–1353
- Lopez-Serra L, Lengronne A, Borges V, Kelly G, Uhlmann F (2012) Budding yeast Wapl controls sister chromatid cohesion maintenance and chromosome condensation. *Curr Biol* 23: 64–69
- Losada A, Hirano M, Hirano T (1998) Identification of *Xenopus* SMC protein complexes required for sister chromatid cohesion. *Genes Dev* 12: 1986–1997
- Losada A, Hirano T (2005) Dynamic molecular linkers of the genome: the first decade of SMC proteins. *Genes Dev* 19: 1269–1287
- Louie E, German J (1981) Roberts's syndrome. II. Aberrant Y-chromosome behavior. *Clin Genet* 19: 71–74
- Lucas I, Palakodeti A, Jiang Y, Young DJ, Jiang N, Fernald AA, Le Beau MM (2007) High-throughput mapping of origins of replication in human cells. *EMBO Rep* 8: 770–777
- Lyons NA, Morgan DO (2011) Cdk1-dependent destruction of Eco1 prevents cohesion establishment after S phase. *Mol Cell* 42: 378–389
- Lyons NA, Fonslow BR, Diedrich JK, Yates JR, Morgan DO (2013) Sequential primed kinases create a damage-responsive phosphodegron on Eco1. *Nat Struct Mol Biol* 20: 194–201
- Maserati E, Pasquali F, Zuffardi O, Buttitta P, Cuoco C, Defant G, Gimelli G, Fraccaro M (1991) Roberts syndrome: phenotypic variation, cytogenetic definition and heterozygote detection. *Ann Genet* 34: 239–246
- Mayer ML, Pot I, Chang M, Xu H, Aneliunas V, Kwok T, Newitt R, Aebersold R, Boone C, Brown GW, Hieter P (2004) Identification of protein complexes required for efficient sister chromatid cohesion. *Mol Biol Cell* 15: 1736–1745
- Michaelis C, Ciosk R, Nasmyth K (1997) Cohesins: chromosomal proteins that prevent premature separation of sister chromatids. *Cell* 91: 35–45
- Minamino M, Ishibashi M, Nakato R, Akiyama K, Tanaka H, Kato Y, Negishi L, Hirota T, Sutani T, Bando M, Shirahige K (2015) Esco1 acetylates cohesin via a mechanism different from that of Esco2. *Curr Biol* 25: 1694–1706
- Moldovan G-L, Pfander B, Jentsch S (2006) PCNA controls establishment of sister chromatid cohesion during S phase. *Mol Cell* 23: 723–732
- Nasmyth K, Schleiffer A (2004) From a single double helix to paired double helices and back. *Philos Trans R Soc Lond B Biol Sci* 359: 99–108
- Nasmyth K (2011) Cohesin: a catenase with separate entry and exit gates? *Nat Cell Biol* 13: 1170–1177
- Nativio R, Wendt KS, Ito Y, Huddleston JE, Uribe-Lewis S, Woodfine K, Krueger C, Reik W, Peters J-M, Murrell A (2009) Cohesin is required for higher-order chromatin conformation at the imprinted IGF2-H19 locus. *PLoS Genet* 5: e1000739
- Nishiyama T, Ladurner R, Schmitz J, Kreidl E, Schleiffer A, Bhaskara V, Bando M, Shirahige K, Hyman AA, Mechtler K, Peters J-M (2010) Sororin mediates sister chromatid cohesion by antagonizing Wapl. *Cell* 143: 737–749
- Panigrahi AK, Zhang N, Otta SK, Pati D (2012) A cohesin-RAD21 interactome. *Biochem J* 442: 661–670
- Peters J-M, Nishiyama T (2012) Sister chromatid cohesion. *Cold Spring Harb Perspect Biol* 4: a011130
- Petronczki M, Chwalla B, Siomos MF, Yokobayashi S, Helmhart W, Deutschbauer AM, Davis RW, Watanabe Y, Nasmyth K (2004) Sister-chromatid cohesion mediated by the alternative RF-CCTf18/Dcc1/Ctf8, the helicase Chl1 and the polymerase-alpha-associated protein Ctf4 is essential for chromatid disjunction during meiosis II. *J Cell Sci* 117: 3547–3559
- Poser I, Sarov M, Hutchins JRA, Hériché J-K, Toyoda Y, Pozniakovskiy A, Weigl D, Nitzsche A, Hegemann B, Bird AW, Pelletier L, Kittler R, Hua S, Naumann R, Augsburg M, Sykora MM, Hofemeister H, Zhang Y, Nasmyth K, White KP et al (2008) BAC TransgeneOmics: a high-throughput method for exploration of protein function in mammals. *Nat Methods* 5: 409–415
- Rahman S, Jones MJK, Jallepalli PV (2015) Cohesin recruits the Esco1 acetyltransferase genome wide to repress transcription and promote cohesion in somatic cells. *Proc Natl Acad Sci USA* 112: 11270–11275
- Rankin S, Ayad NG, Kirschner MW (2005) Sororin, a substrate of the anaphase-promoting complex, is required for sister chromatid cohesion in vertebrates. *Mol Cell* 18: 185–200
- Rao SSP, Huang S-C, Glenn St Hilaire B, Engreitz JM, Perez EM, Kieffer-Kwon K-R, Sanborn AL, Johnstone SE, Bascom GD, Bochkov ID, Huang X, Shamim MS, Shin J, Turner D, Ye Z, Omer AD, Robinson JT, Schlick T, Bernstein BE, Casellas R et al (2017) Cohesin loss eliminates all loop domains. *Cell* 171: 305–320.e24
- Rowland BD, Roig MB, Nishino T, Kurze A, Uluocak P, Mishra A, Beckouët F, Underwood P, Metson J, Imre R, Mechtler K, Katis VL, Nasmyth K (2009) Building sister chromatid cohesion: smc3 acetylation counteracts an antiestablishment activity. *Mol Cell* 33: 763–774
- Samora CP, Saksouk J, Goswami P, Wade BO, Singleton MR, Bates PA, Lengronne A, Costa A, Uhlmann F (2016) Ctf4 links DNA replication with sister chromatid cohesion establishment by recruiting the Chl1 helicase to the replisome. *Mol Cell* 63: 371–384
- Schmidt D, Wilson MD, Spyrou C, Brown GD, Hadfield J, Odom DT (2009) ChIP-seq: using high-throughput sequencing to discover protein-DNA interactions. *Methods* 48: 240–248
- Schmitz J, Watrin E, Lenart P, Mechtler K, Peters J-M (2007) Sororin is required for stable binding of cohesin to chromatin and for sister chromatid cohesion in interphase. *Curr Biol* 17: 630–636

- Schüle B, Oviedo A, Johnston K, Pai S, Francke U (2005) Inactivating mutations in ESCO2 cause SC phocomelia and Roberts syndrome: no phenotype-genotype correlation. *Am J Hum Genet* 77: 1117–1128
- Schwarzer W, Abdennur N, Goloborodko A, Pekowska A, Fudenberg G, Loe-Mie Y, Fonseca NA, Huber W, Haering CH, Mirny L, Spitz F (2017) Two independent modes of chromatin organization revealed by cohesin removal. *Nature* 551: 51–56
- Siddiqui K, On KF, Diffley JFX (2013) Regulating DNA replication in eukarya. *Cold Spring Harb Perspect Biol* 5: a012930
- Sirbu BM, Couch FB, Feigerle JT, Bhaskara S, Hiebert SW, Cortez D (2011) Analysis of protein dynamics at active, stalled, and collapsed replication forks. *Genes Dev* 25: 1320–1327
- Sirbu BM, Couch FB, Cortez D (2012) Monitoring the spatiotemporal dynamics of proteins at replication forks and in assembled chromatin using isolation of proteins on nascent DNA. *Nat Protoc* 7: 594–605
- Skibbens RV, Corson LB, Koshland D, Hieter P (1999) Ctf7p is essential for sister chromatid cohesion and links mitotic chromosome structure to the DNA replication machinery. *Genes Dev* 13: 307–319
- Song J, Lafont A, Chen J, Wu FM, Shirahige K, Rankin S (2012) Cohesin acetylation promotes sister chromatid cohesion only in association with the replication machinery. *J Biol Chem* 287: 34325–34336
- Spyrou C, Stark R, Lynch AG, Tavaré S (2009) BayesPeak: Bayesian analysis of ChIP-seq data. *BMC Bioinformatics* 10: 299
- Ström L, Karlsson C, Lindroos HB, Wedahl S, Katou Y, Shirahige K, Sjögren C (2007) Postreplicative formation of cohesion is required for repair and induced by a single DNA break. *Science* 317: 242–245
- Sutani T, Kawaguchi T, Kanno R, Itoh T, Shirahige K (2009) Budding yeast Wpl1(Rad61)-Pds5 complex counteracts sister chromatid cohesion-establishing reaction. *Curr Biol* 19: 492–497
- Tachibana-Konwalski K, Godwin J, van der Weyden L, Champion L, Kudo NR, Adams DJ, Nasmyth K (2010) Rec8-containing cohesin maintains bivalents without turnover during the growing phase of mouse oocytes. *Genes Dev* 24: 2505–2516
- Tanaka K, Hao Z, Kai M, Okayama H (2001) Establishment and maintenance of sister chromatid cohesion in fission yeast by a unique mechanism. *EMBO J* 20: 5779–5790
- Tedeschi A, Wutz G, Huet S, Jaritz M, Wuensche A, Schirghuber E, Davidson IF, Tang W, Cisneros DA, Bhaskara V, Nishiyama T, Vaziri A, Wutz A, Ellenberg J, Peters J-M (2013) Wapl is an essential regulator of chromatin structure and chromosome segregation. *Nature* 501: 564–568
- Terret M-E, Sherwood R, Rahman S, Qin J, Jallepalli PV (2009) Cohesin acetylation speeds the replication fork. *Nature* 462: 231–234
- Tomkins D, Hunter A, Roberts M (1979) Cytogenetic findings in Roberts-SC phocomelia syndrome(s). *Am J Med Genet* 4: 17–26
- Tóth A, Ciosk R, Uhlmann F, Gálová M, Schleiffer A, Nasmyth K (1999) Yeast cohesin complex requires a conserved protein, Eco1p(Ctf7), to establish cohesion between sister chromatids during DNA replication. *Genes Dev* 13: 320–333
- Uhlmann F, Nasmyth K (1998) Cohesion between sister chromatids must be established during DNA replication. *Curr Biol* 8: 1095–1101
- Unal E, Heidinger-Pauli JM, Koshland D (2007) DNA double-strand breaks trigger genome-wide sister-chromatid cohesion through Eco1 (Ctf7). *Science* 317: 245–248
- Unal E, Heidinger-Pauli JM, Kim W, Guacci V, Onn I, Gygi SP, Koshland DE (2008) A molecular determinant for the establishment of sister chromatid cohesion. *Science* 321: 566–569
- Van Den Berg DJ, Francke U (1993) Roberts syndrome: a review of 100 cases and a new rating system for severity. *Am J Med Genet* 47: 1104–1123
- Vega H, Waisfisz Q, Gordillo M, Sakai N, Yanagihara I, Yamada M, van Gosliga D, Kayserili H, Xu C, Ozono K, Jabs EW, Inui K, Joenje H (2005) Roberts syndrome is caused by mutations in ESCO2, a human homolog of yeast ECO1 that is essential for the establishment of sister chromatid cohesion. *Nat Genet* 37: 468–470
- Warbrick E (1998) PCNA binding through a conserved motif. *BioEssays* 20: 195–199
- Webb B, Sali A (2014) Comparative protein structure modeling using MODELLER. *Curr Protoc Bioinformatics* 47: 5.6.1–32
- Whelan G, Kreidl E, Peters J-M, Eichele G (2012a) The non-redundant function of cohesin acetyltransferase Esco2: some answers and new questions. *Nucleus* 3: 330–334
- Whelan G, Kreidl E, Wutz G, Egner A, Peters J-M, Eichele G (2012b) Cohesin acetyltransferase Esco2 is a cell viability factor and is required for cohesion in pericentric heterochromatin. *EMBO J* 31: 71–82
- Williams BC, Garrett-Engle CM, Li Z, Williams EV, Rosenman ED, Goldberg ML (2003) Two putative acetyltransferases, san and deco, are required for establishing sister chromatid cohesion in *Drosophila*. *Curr Biol* 13: 2025–2036
- Wutz G, Várnai C, Nagasaka K, Cisneros DA, Stocsits R, Tang W, Schoenfelder S, Jessberger G, Muhar M, Hossain JM, Walther N, Koch B, Kueblbeck M, Ellenberg J, Zuber J, Fraser P, Peters JM (2017) CTCF, WAPL, and PDS5 proteins control the formation of TADs and loops by cohesin. *EMBO J* 36: 3573–3599
- Yeeles JTP, Deegan TD, Janska A, Early A, Diffley JFX (2015) Regulated eukaryotic DNA replication origin firing with purified proteins. *Nature* 519: 431–435
- Yeeles JTP, Janska A, Early A, Diffley JFX (2017) How the eukaryotic replisome achieves rapid and efficient DNA replication. *Mol Cell* 65: 105–116
- Yoda K, Kitagawa K, Masumoto H, Muro Y, Okazaki T (1992) A human centromere protein, CENP-B, has a DNA binding domain containing four potential alpha helices at the NH2 terminus, which is separable from dimerizing activity. *J Cell Biol* 119: 1413–1427
- Zhang J, Shi X, Li Y, Kim B-J, Jia J, Huang Z, Yang T, Fu X, Jung SY, Wang Y, Zhang P, Kim S-T, Pan X, Qin J (2008) Acetylation of Smc3 by Eco1 is required for S phase sister chromatid cohesion in both human and yeast. *Mol Cell* 31: 143–151